Selective ligands for Na$^+$/K$^+$-ATPase α isoforms differentially and cooperatively regulate excitability of pyramidal neurons in distinct brain regions

Darpan Chakraborty [a], Olga V. Fedorova [b], Alexei Y. Bagrov [b], Hanoch Kaphzan [a, *]

[a] Sagol Department of Neurobiology, University of Haifa, Haifa, Israel
[b] National Institute on Aging, NIH, Baltimore, MD, USA

ABSTRACT

Sodium-potassium ATPase (NaKA) is a plasma membrane enzyme responsible for influencing membrane physiology by direct electrogenic activity. It determines cellular excitability and synaptic neurotransmission, thus affecting learning and memory processes. A principle catalytic α subunit of NaKA has development-specific expression pattern. There are two α isoforms, α1 and α3, in adult brain neurons. Although NaKA is a housekeeping enzyme, the physiological differences between these two α isoforms in different brain regions have not been well explored. Endogenous cardiotonic steroids, including Marinobufagenin and Ouabain, control the cell homeostasis and cell functions *via* inhibiting NaKA. Here we employed selective inhibition of α1 and α3 NaKA isoforms by Marinobufagenin and Ouabain respectively, to measure the contribution of α subunits in cellular physiology of three distinct mouse brain regions. The results of the whole cell recording demonstrated that α1 isoform predominated in layer-5 pyramidal cells at rostral motor cortex, while α3 isoform governed the pyramidal neurons at hippocampal CA1 region and to a lesser extent the layer-5 pyramidal neurons of parietal cortex. Furthermore, selective α isoform inhibition induced differential effects on distinct physiological properties even within the same brain region. In addition, our results supported the existence of synergism between two NaKA α isoforms. To conclude, this systematic study of NaKA α isoforms demonstrated their broader roles in neuronal functioning in a region-specific manner.

© 2017 Elsevier Ltd. All rights reserved.

1. Introduction

Na/K-ATPase (NaKA) is a unique enzyme, which controls the active transport of Na$^+$ and K$^+$ ions across the membrane. As a major housekeeping protein, it contributes to the maintenance of cellular homeostasis, transmembrane resting potential, cellular volume and intracellular osmolarity. Due to this, NaKA utilizes approximately 50% of the cell's energy consumption (Ames, 2000; Attwell and Laughlin, 2001; Erecińska and Silver, 1994; Howarth et al., 2012). There is a large body of evidence suggesting that NaKA activity in the nervous system regulates various brain functions such as enabling additional data coding and subsequent information processing (Forrest, 2014; Forrest et al., 2012). In addition to its function as an ion pump and enzyme, NaKA is a receptor and the only known target for the endogenous cardiotonic steroids (CTS), which include bufadienolide marinobufagenin (MBG) and cardenolide ouabain (Oua) (Bagrov et al., 2009; Fedorova et al., 2007, 2002).

Structurally, NaKA is a heterodimeric integral membrane protein comprised of α (100 kDa) subunit and β (55 kDa) subunit and sometimes is accompanied by a third regulatory protein, FXYD. The number of α subunits is a key determining factor for the expression and activity of NaKA (DeTomaso et al., 1994; Laughery et al., 2007; Lescale-Matys et al., 1993; McDonough and Farley, 1993; Mircheff et al., 1992; Tokhtaeva et al., 2009). There are three α isoforms (α1, α2, α3) which are differentially expressed in various organs. α1 subunit is a housekeeping protein and is expressed in most of the cell types and body organs. α1 is often the only subunit present in the whole tissue, like in erythrocytes, kidney epithelia and liver cells, but in skeletal, cardiac and smooth muscles α2 is also expressed. However, the nervous system expresses all three

subunits (Blanco and Mercer, 1998; Herrera et al., 1987; Lingrel JB, 1992; Moeller et al., 2011). Interestingly, in the adult rodent brain, α isoform expression varies among specific cell types; α2 is exclusively expressed in astrocytes, α3 is restricted to neurons and α1 is widely present in both glia and neurons. Therefore, neurons in the adult rodent brain comprise of the two most prevalent isoforms, α1 and α3. The significance of distinctive expression profile of different isoforms in the brain is not well understood. Functionally, these two isoforms have different affinity for various ligands, including CTS NaKA inhibitors, MBG and Oua (Fedorova and Bagrov, 1997). For example, α1 has a higher affinity for Na^+ ions than α3 isoform (Azarias et al., 2013; Munzer et al., 1994; Zahler et al., 1997). Moreover, endogenous forms of these two CTS participate in two major pathways: the ionic pathway, which is initiated by inhibition of NaKA activity, and the signaling pathway, which requires binding of CTS to NaKA and does not necessarily involve sodium pump inhibition (Bagrov et al., 2009). There are numerous studies which also confirm that each isoform haploinsufficiency leads to discrete behavioral phenotypes (Lingrel et al., 2007; Moseley et al., 2007). Yet the functional importance of such α isoform diversity in the brain is unresolved.

It has been reported that inhibition of NaKA activity with Oua can have varied effects in different brain regions (Forrest, 2014). These differential effects were hypothetically attributed to the diverse expression profile of NaKA α isoforms (Forrest, 2014). Taken together, these findings emphasize the necessity of investigation of the distinct cellular physiology of the two most predominant neuronal NaKA isoforms α1 and α3, in different brain areas. In addition, understanding the unique physiology of NaKA isoforms in various brain regions is crucial because NaKA is implicated in numerous neuropsychiatric disorders such as autism spectrum disorders (Al-Mosalem et al., 2009; Ji et al., 2009; Kaphzan et al., 2013, 2011), schizophrenia (Corti et al., 2011), affective disorders (Chetcuti et al., 2008; Goldstein et al., 2006) and others.

In the present study, we have focussed on delineating the physiological differences between α1 and α3 isoforms *via* selective pharmacological inhibition with treatment of MBG and Oua respectively. Oua exhibits much higher affinity to rodent α3 NaKA than to α1 (Fedorova and Bagrov, 1997; Jamme et al., 1997). In contrast, MBG binds to rodent α1 with higher affinity than to α3 NaKA (Bagrov et al., 2009; Fedorova and Bagrov, 1997). To test the hypothesis that MBG and Oua have different effects on these two NaKA isoforms in different areas of the brain, we examined excitatory pyramidal neurons from three distinct mouse brain regions: hippocampal CA1 Stratum Pyramidale (CA1), posterior parietal cortex layer-5 (PTL) from the posterior (caudal) brain and, primary motor cortex layer-5 (MO) from anterior (rostral) brain region (see Supp. Fig. 1) in response to MBG and Oua. In this study, we investigated differential physiological effects of selective NaKA isoform inhibition in the aforementioned selected mouse brain areas using whole-cell patch clamp recording.

2. Materials and methods

2.1. Animals

For all experiments we used, C57BL/6 mice 10—12 weeks of age of both genders. Experimental procedures were performed in accordance with National Institutes of Health guidelines and were approved by the University of Haifa animal ethics committee.

2.2. Brain regions identification

Coronal brain slices were obtained following the identification of brain region morphology based on the Allen Institute mouse

brain reference atlas (Allen Institute for Brain Science. Webpage; Lein et al., 2007). CA1sp recorded in this study was located on the coronal slices taken 2.4—3.2 mm posterior to the bregma. MOpL5 was recorded from coronal slices 1.3 mm anterior to 0.8 mm posterior to the bregma. The larger striatum and starting point of the hippocampus were used as landmarks for locating the end of MOpL5. PTLpL identification was based on the images of slices positioned at 1.6—2.1 mm posterior to the bregma.

2.3. Tissue preparation

Mice were sacrificed by cervical dislocation, and 300 μm coronal brain slices were cut with a Ci 7000 smz2 (Campden Instruments, UK) in ice-cold (~4 °C) cutting solution containing (in mM) 110 sucrose, 60 NaCl, 3 KCl, 1.25 NaH_2PO_4, 28 $NaHCO_3$, 0.5 $CaCl_2$, 7 $MgCl_2$ and 5 glucose. Slices were recovered for 30 min at 37 °C in artificial cerebrospinal fluid (ACSF) containing (in mM) 125 NaCl, 2.5 KCl, 1.25 NaH_2PO_4, 25 $NaHCO_3$, 25 D-glucose, 2 $CaCl_2$, and 1 $MgCl_2$ ACSF, with an additional recovery for 30 min at room temperature. After initial recovery, slices were placed in a submerged chamber at 35 °C in ACSF (>2 mL/min) and incubated for no less than 30 min before patching occurred; the slices were maintained in these conditions for duration of the experiment. All solutions were constantly carboxygenated with 95% O_2 + 5% CO_2.

2.4. Current clamp whole-cell recording

Pyramidal cells were both visually and electrophysiologically identified as previously described (Chen et al., 1996; Christophe et al., 2005; Colbert and Levy, 1992; Franceschetti et al., 1993; Lacaille et al., 1987; Schubert et al., 2001; Staff et al., 2000). Brain slices were illuminated and visualized with an infrared differential interference contrast microscope (BX51-WI; Olympus, USA) with a 60× water-immersion objective mounted on a fixed-stage. The image was displayed on a video monitor using a charge-coupled device camera (DAGE-MTI, USA). Recordings were amplified by multiclamp 700B and digitized by Digidata 1440 (Molecular Devices, California, USA). The recording electrode was pulled from a borosilicate glass pipette (3—5 MΩ) using an electrode puller (P-1000; Sutter Instruments, USA) and filled with a K-gluconate-based internal solution containing (in mM) 130 K-gluconate, 5 KCl, 10 HEPES, 2 MgCl2, 0.6 EGTA, 2 Mg-ATP, 0.5 Na_3-GTP, osmolarity 290 mOsm, and pH 7.3. Recording glass pipettes were patched onto the pyramidal cells soma region. Voltages for liquid junction potential (+8 mV) were corrected offline. All intrinsic properties were recorded in current clamp mode. For equilibration, recordings of baseline in ACSF without inhibitors started 10 min after entering whole cell mode. All current-clamp recordings were low-pass filtered at 10 kHz and sampled at 50 kHz. Series resistance was compensated and only series resistance <20 MΩ was included in the data set. Pipette capacitance was ~99% compensated. The method of measuring active intrinsic properties was based on a modified version of a previously described procedure (Kaphzan et al., 2013, 2011).

To study the biophysical property of membrane, resting membrane potential (Rp) was measured 10 min after the seal was ruptured. The sag potential was measured from the inward rectification at hyperpolarized membrane potentials obtained by injecting negative current square pulse (−100 pA, 1s). The input resistance (IR) was calculated from the current-voltage relationship at the linear portion of voltage responses to steps of hyperpolarizing current pulses (−150 to 0 pA, 1s). In the case of a single action potential (AP) parameter, after an initial assessment of the current, which was required to induce an AP at the start of current injection with large steps (50 pA), we injected a series of brief

depolarizing currents for 10 ms in steps of 10 pA increments. The first AP that appeared at the 5 ms time point was analyzed. A curve of dV/dt was created for that trace, and the threshold was considered as the 30 V/s point on the rising slope of an action potential (Kaphzan et al., 2013, 2011). The AP amplitude was measured from the threshold point to the spike peak, while the AP duration was measured at the point of half-amplitude of the spike. The area under the curve (AUC) was measured for each AP; total area from threshold to the equipotential point in repolarizing curve was analyzed.

The medium afterhyperpolarization (mAHP) was measured using prolonged (3s), high-amplitude (3 nA) somatic current injections to initiate time-locked AP trains of 50 Hz frequency and duration (10–50 Hz, 1 or 3 s) in pyramidal cells. mAHP was measured from the equipotential point of resting potential to the anti-peak of the same spike (Gulledge et al., 2013; Landfield and Pitler, 1984; Oh et al., 2010; Power et al., 2002; Wu et al., 2004).

AP firing frequency was measured by counting the number of APs generated due to current injections of 1000 ms square current pulses in 50 pA steps from 0 pA to 300 pA.

Recordings of pyramidal cells from all three brain regions were performed on the same day, from the same animal and with same stock of NaKA inhibitors. As these antagonists are not readily washable, we recorded only one neuron per slice to be assertive that lingering NaKA blockade was not contributing to our results. The slice was removed and the chamber and tubing were thoroughly washed after each cell recording.

2.5. Voltage clamp whole-cell recording

For the synaptic current measurement, EPSCs were recorded in voltage clamp, at a holding potential of −70 mV using the same K-Gluconate based internal solution used for current-clamp recording. For synaptic input, a bipolar electrode was used to stimulate either the Schaffer collateral for the recording of CA1sp or layer 2–3 for cortical layer 5 pyramidal cells. For equilibration, recordings were started 10 min after entering the whole cell mode. All voltage-clamp recordings were low-pass filtered at 10 kHz and sampled at 50 kHz. Series resistance was 90% compensated. Series resistance, input resistance, and membrane capacitance were monitored during the entire experiment. Data exclusion criteria were based on changes in the above parameters of more than 15% from the baseline.

2.6. NaKA inhibitors application

MBG was prepared as previously described (Fedorova and Bagrov, 1997) and Oua was purchased from Sigma, Israel. To determine the effects of selective inhibition of α1NaKA or α3NaKA subunits, we bath applied either MBG (1 μM) or Oua (1 μM) dissolved in ACSF. We also examined the combined effects of both drugs (MBG 1 μM + Oua 1 μM). Concentrations of MBG and Oua were based on the results of previous publications. Briefly, in rodent brains, the affinity of Oua for α3-NaKA is 25-fold higher than its affinity for α1-NaKA (Fedorova and Bagrov, 1997). Moreover, the IC_{50} of Oua for rodent brain α1, α2, and α3 NaKA isoforms are 1.3 mM, 4.5 μM and 2.9 nM, respectively (Jamme et al., 1997). Therefore, Oua dissolved in ACSF, was perfused in the brain slices at a concentration of 1 μM to inhibit α3 without affecting the α1 isoform. MBG affinity for rodent α1-NaKA is 53-fold higher than the affinity for α3-NaKA (Fedorova and Bagrov, 1997). The IC_{50} concentration needed for inhibition of rodent α3 NaKA by Oua and α1 NaKA by MBG are nearly similar (2.6 nmol/L and 2.1 nmol/L, respectively) (Fedorova and Bagrov, 1997). Considering these results, 1 μM of MBG dissolved in ACSF was used to perfuse the brain

slices. In order to achieve maximal slice penetration of the drugs and to reach a steady state, whole cell recordings with inhibitors were performed 20 min after bath application of the inhibitors.

2.7. Statistical analysis

Calculated statistical values in the Figures, Tables, and text are presented as means ± S.E.M. Differences in mean values were assessed with One-way repeated-measures ANOVA followed by multiple comparisons correction using Bonferroni post-hoc tests, or a Two-way repeated-measures ANOVA followed by multiple comparisons correction using Tukey's post-hoc tests, whenever appropriate. A comparison between the drugs within each region for each induced effect was statistically evaluated as the interaction between the type of drug and the change it induced, while comparing before and after treatment (pre-post). All statistical comparisons included the group with the combined treatment of MBG and Oua as well. Differences between means were considered statistically significant if p < 0.05. All statistical analysis was performed with IBM-SPSS 21 and GraphPad Prism 7 software.

3. Results

In the herein study, we examined the whole cell recording of 57, 33 and 37 pyramidal cells from caudal brain regions, the hippocampus (CA1sp) and the parietal cortex (PTLpL5), and the rostral brain region of primary motor cortex (MOpL5) respectively (Supplementary Fig. 1). It was demonstrated that these three brain regions display significant differences in the basal state passive and active intrinsic properties (Table 1).

Pyramidal cells in CA1 and MO regions showed clear differential responses to both α1 or α3 NaKA inhibition. However, pyramidal cells in PTL region showed either a trend to respond like those found in the CA1 or equivocal responses to inhibition of the two NaKA isoforms. Therefore, for the sake of clarity, PTL data is mentioned briefly, and the main comparison is drawn between CA1 and MO regions.

We have demonstrated that MBG (1 μM) or Oua (1 μM) selectively inhibited α1 or α3 isoforms respectively. Further, we have found that application of Oua 10 μM in CA1 or MBG 10 μM in MO region produced similar or stronger effects in comparison with the combination of these two CTS simultaneously at the concentration of 1 μM each (Supp. Fig 2–3).

3.1. Isoform-selective NaKA inhibition exhibited differential effects on passive properties in different brain regions

Because NaKA is a major contributor in the maintenance of the passive properties of the brain, its inhibition may depolarize resting membrane potential (Baylor and Nicholls, 1969; Glitsch, 2001; Pulver and Griffith, 2010; Wang et al., 2012). We sought to measure the efficacy of these CTS in the selected brain regions. Besides measuring the major passive properties as resting membrane potential (RP) and input resistance (IR), we measured the hyperpolarization-activated cation current (I_h- Current) or sag potential (SP). The previous study on central pattern generator neurons of leeches showed the interaction of NaKA pump with I_h current (Kueh et al., 2016). Our study showed in CA1; MBG induced a meager depolarization of RP and an increase of IR (p < 0.0001 for both, RM-ANOVA), but failed to alter SP (p = 0.085, RM-ANOVA) (Fig. 1). On the other hand, Oua in CA1 also induced a depolarization of RP and an increase of IR (p < 0.0001 for both, RM-ANOVA); however, it also induced a significant reduction of SP (p < 0.0001, RM-ANOVA) (Fig. 1). In MO region, MBG depolarized RP, increased IR and decreased SP (p < 0.0001, 0.005 and p < 0.0001 respectively,

Table 1
Cellular electrophysiological properties in selected three brain regions.

Rp, IR and Sag Potential			
	CA1sp	PTLpL5	MOpL5
Rp (mV)	−62.59 ± 0.29 (57) €¥	−70.07 ± 0.41 (33) $	−68.54 ± 0.47 (37)
IR (mΩ)	135.233 ± 3.59 (57) €	191.47 ± 8.78 (33) $	153.15 ± 6.94 (37)
Sag Potential (mV)	3.04 ± 0.1 (57) ¥	3.1 ± 0.19 (33) $	1.93 ± 0.06 (37)
Single AP parameters			
	CA1sp	PTLpL5	MOpL5
AP threshold (mV)	−44.10 ± 0.50 (57)	−43.48 ± 0.51 (33)	−44.17 ± 0.75 (37)
AP Amplitude (mV)	82.66 ± 0.75 (57) ¥	83.39 ± 1.64(33)	87.18 ± 1.57 (37)
AP dV/dt (mV/msec.)	358.27 ± 8.28 (57) €¥	292.34 ± 7.08 (33) $	420.40 ± 16.77 (37)
AP width (msec.)	0.80 ± 0.01 (57) €¥	0.93 ± 0.02 (33) $	0.72 ± 0.01 (37)
AP AUC (mV × msec)	132.81 ± 4.07 (57) ¥	125.79 ± 2.60 (33) $	100.55 ± 1.35 (37)
AHP (mV)	−6.53 ± 0.37 (45)	−5.47 ± 0.44 (33)	−5.80 ± 0.38 (33)

Data are presented as means ± SEM (n, number of cells). € CA1sp significantly different from PTLpL5, ¥ CA1sp significantly different from MOpL5, $ PTLpL5 significantly different from MOpL5 (P < 0.05, One Way ANOVA with Bonferroni post-hoc test).

RM-ANOVA), while Oua did not affect these passive intrinsic properties (p = 0.339, p = 0.982, and p = 0.506 respectively, RM-ANOVA) (Fig. 1). PTL showed similar responses to CA1 concerning these intrinsic properties (Fig. 1) (see Table 2). In a further comparison of the interaction between drugs and their effects within each brain region (interaction: drug × pre-post), it was evident that the effects of Oua were significantly stronger than those of MBG in CA1; while in the MO region, we observed more dominant effects of MBG. This was especially evident when the responses of RP depolarization and SP reduction to MBG or Oua application were compared (Fig. 1). In CA1 Oua had a stronger effect than MBG in depolarizing the RP and reducing the SP (p < 0.05 and p < 0.001 respectively, 2-way RM-ANOVA), while MBG had a stronger effects on RP and SP in the MO region (p < 0.05 and p < 0.001 respectively, 2-way RM-ANOVA) (Fig. 1). In addition, the effects of Oua on RP and SP in CA1 were not different from the combination of two drugs, and similarly, the effects of MBG on RP and SP in MO region also were not different in comparison with the combined effect of two drugs (Fig. 1). To conclude, although these two drugs seem to have a similar direction of effects on the passive intrinsic properties, it appears that α3-NaKA has a more prevalent role in CA1, while α1-NaKA plays a dominant role in MO.

Similar comparisons between Oua and MBG in the PTL region showed no differences between MBG and Oua (Fig. 1) (for comparisons between drugs see Table 3).

3.2. Specific NaKA subunit inhibition in different brain regions exhibited differential effects on action potential (AP) properties

Because the maximum pump current usually is not generated at rest, a certain amount of residual pump current is used in high cellular activity (Mogul et al., 1990; Sakai et al., 1996). Next, to measure the effect of selective NaKA isoforms inhibition on maximum pump current, next, we characterized the active intrinsic properties. Our results showed that Oua in the CA1 increased the threshold potential (TP), altered AP shape by reducing the amplitude and broadening the width, thus reduced the AP rate of rise, and prompted a net effect of increasing the area under the curve (AUC) (p < 0.0001 for all, RM-ANOVA) (Fig. 2). In contrast, Oua did not alter any of these active intrinsic properties in the MO.

On the other hand, MBG in MO increased threshold potential (TP), reduced AP amplitude and broadened the width, reduced AP rate of rise, and induced an overall increase of the AP's AUC (p < 0.05 for TP and p < 0.0001 for all others, RM-ANOVA) (Fig. 2). However, in CA1, MBG failed to broaden the AP width and did not increase the AP's AUC (p = 0.094 and p = 0.305 respectively, RM-

ANOVA) (Fig. 2) (see Table 2).

In addition to the regional differences, a comparison between two drugs regarding the extent of the effects they induced within each region (interaction drug × pre-post), demonstrated that in CA1, Oua had a more robust impact than MBG in increasing TP, reducing AP amplitude, broadening AP width, reducing AP rate of rise, and increasing AP's AUC (p < 0.05, p < 0.01, p < 0.0001, p < 0.05 and p < 0.0001 respectively, 2-way RM-ANOVA). In contrast, in the MO region, MBG had a stronger effect than Oua in reducing AP amplitude, broadening AP width, reducing AP rate of rise, and increasing AP's AUC (p < 0.01, p < 0.0001, p < 0.001 and p < 0.0001 respectively, 2-way RM-ANOVA). Interestingly, there was no significant difference between MBG and Oua in the MO in increasing the TP. Taken together; these two drugs had comparable effects on active intrinsic properties. But like passive properties, α3-NaKA played a more prevalent role in CA1, while α1-NaKA was predominant in MO. In contrast, a comparison between Oua and MBG in PTL region showed no disparity concerning the alteration of the active intrinsic properties (Fig. 2) (For comparisons between the drugs see Table 3).

3.3. NaKA subunit specific inhibition differentially decreased mAHP in selected brain regions

mAHP is a hyperpolarizing current that occurs after spiking activity (Guan et al., 2015; Gulledge et al., 2013; King et al., 2015; Lacaille et al., 1987), and it is primarily mediated by the Ca^{2+}-dependent K^+ channel and voltage-gated K^+ conductance (Giese et al., 1998; Gulledge et al., 2013; Schwindt et al., 1988). We determined mAHP following a train of APs (Gulledge et al., 2013; Landfield and Pitler, 1984; Oh et al., 2010). In agreement with previous results, we observed Oua induced a reduction of mAHP in CA1, but did not alter mAHP in MO (p < 0.0001 and p = 0.109 respectively, RM-ANOVA) (Fig. 3). Conversely, MBG reduced mAHP in MO but did not affect mAHP in CA1 (p < 0.0001 and p = 0.334 respectively, RM-ANOVA) (Fig. 3, see Table 2). A comparison between two drugs regarding mAHP alteration (interaction: drug × pre-post) showed that Oua had a significantly stronger effect in CA1, and MBG had a considerably more robust impact in MO region (p < 0.01 and p < 0.0001 respectively, 2-way RM-ANOVA). Furthermore, this comparison demonstrated that Oua effect was similar to the effect induced by combination of Oua and MBG in CA1, and correspondingly MBG's effect is similar to the effect induced by Oua and MBG combination in MO (Fig. 3). Alternatively, effect of MBG on mAHP in CA1 was significantly different compared to the combination of two drugs, which is similar for Oua effect in
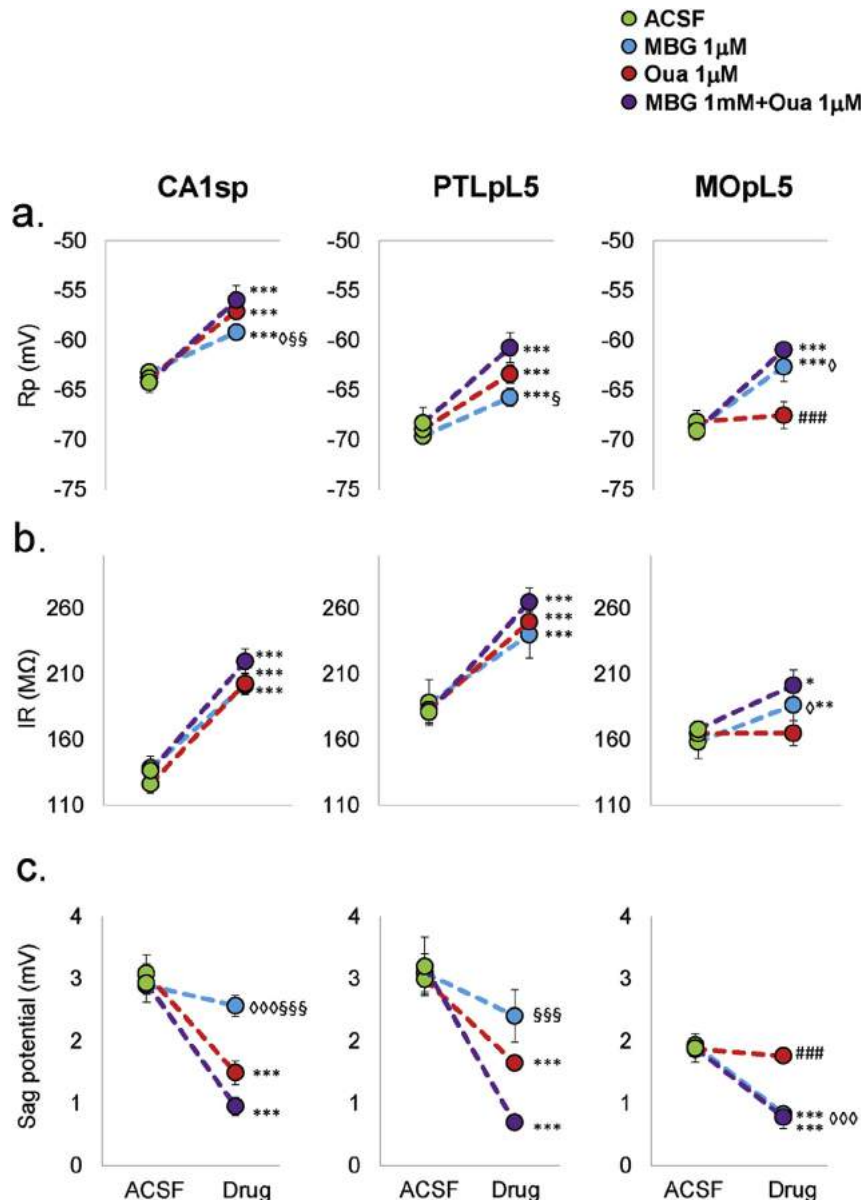
Fig. 1. NaKA inhibition alters passive membrane properties. **(a)** In CA1sp and PTLpL5; MBG, Oua and Comb significantly depolarize the Rp from ACSF (Left and Middle). Notably, in CA1 and PTLpL5, the effect of MBG is considerably less than the Oua and Comb effect (Left and Middle). While in MOpL5, Oua does not alter the Rp than ACSF but MBG and Comb significantly depolarizes it thus the effect of Oua is significantly less than the effect of MBG and Comb (Right). **(b)** NaKA inhibition significantly increases IR than ACSF in all three regions to a similar extent, except in MOpL5, where Oua does not alter the IR than ACSF. Moreover, the effect of MBG is different from the effect of Oua (Right). **(c)** Oua and Comb significantly reduce Sag Potential in CA1sp and PTLpL5 than ACSF. While MBG and Comb do the same in MOpL5. The effect of MBG is significantly different than Comb in CA1sp and PTLpL5 (Left and Middle), while in the MOpL5 effect of Oua is different than the effect of MBG and Comb (Right). All analysis was done by repeated measure ANOVA, multiple comparisons Tukey Corrections with $p < 0.05$ (Detailed in Tables 2 and 3) and the values in the graphs are Mean ± SEM. The effect of drug different than ACSF (green) *($p < 0.05$), **($p < 0.01$), ***($p < 0.001$). The difference between the effect of MBG (blue) and Oua (red) shown with ◊($p < 0.05$), ◊◊($p < 0.01$) and ◊◊◊($p < 0.001$). §($p < 0.05$), §§($p < 0.01$) and §§§($p < 0.001$) shows the effect of MBG (blue) and Comb (purple) are different. While #($p < 0.05$), ##($p < 0.01$) and ###($p < 0.001$) used to show the significant difference between effect of Oua and Comb.

the MO (Fig. 3, Table 3). Comparison between effects on mAHP after Oua or MBG application in PTL region showed no differences (Fig. 3). Again, it is apparent that α3-NaKA is more prevalent in CA1, as α1-NaKA is at MO.

3.4. Selective inhibition of NaKA subunit in different brain regions induced a differential bimodal excitability alteration

All pyramidal cells in this study fired rhythmically in response to incremental depolarizing current injections and were regular spiking (RS) cells (Agmon and Connors, 1991; Chagnac-Amitai et al.,

1990). The correlation of firing frequency to the injected current is termed FI-curve. In agreement with the above mentioned results, we observed that Oua induced a reduction (right shift) in the FI curve at CA1, while the FI curve was unaffected in the MO region ($p < 0.001$ and $p = 0.69$ respectively, RM ANOVA) (see Table 2). Nevertheless, the Oua induced reduction in the FI curve at CA1 was weaker than the one observed by the combination of drugs ($p < 0.001$, 2-way RM-ANOVA) (Fig. 4). Surprisingly, in CA1, contrary to previous results where MBG showed similar but much weaker effects than Oua, MBG induced an increase (left shift) in FI curve ($p < 0.001$, RM-ANOVA), while in MO, MBG almost entirely

Table 2
Differential NaKA inhibition alters electrophysiological properties.

Property [RM-ANOVA, Sphericity Assumed]	drug	CA1sp	PTLpL5	MOpL5
Rp (mV)	MBG	↑p < 0.0001(n = 26)	↑p < 0.0001(n = 10)	↑p < 0.0001(n = 14)
CA1: [pre-post F(1, 54) = 272.7, p < 0.0001]	Oua	↑p < 0.0001(n = 21)	↑p < 0.0001(n = 15)	p = 0.339(n.s) (n = 14)
PTL: [pre-post F(1, 30) = 160.1, p < 0.0001]	Comb	↑p < 0.0001(n = 10)	↑p < 0.0001(n = 8)	↑p < 0.0001(n = 9)
MO: [pre-post F(1, 34) = 124.9, p < 0.0001]				
IR (mΩ)	MBG	↑p < 0.0001(n = 26)	↑p < 0.001(n = 10)	↑p < 0.005(n = 14)
CA1: [pre-post F(1, 54) = 198.4, p < 0.0001]	Oua	↑p < 0.0001(n = 21)	↑p < 0.0001(n = 15)	p = 0.982(n.s) (n = 14)
PTL: [pre-post F(1, 30) = 69.00, p < 0.0001]	Comb	↑p < 0.0001(n = 10)	↑p < 0.0001(n = 8)	↑p < 0.05(n = 9)
MO: [pre-post F(1, 34) = 9.594, p = 0.004]				
Sag (mV)	MBG	p = 0.085(n.s) (n = 26)	p = 0.053(n = 10)	↓p < 0.0001(n = 14)
CA1: [pre-post F(1, 54) = 86.93, p < 0.0001]	Oua	↓ p < 0.0001(n = 21)	↓p < 0.0001(n = 15)	p = 0.506(n.s) (n = 14)
PTL: [pre-post F(1, 30) = 59.74, p < 0.0001]	Comb	↓ p < 0.0001(n = 10)	↓p < 0.0001(n = 8)	↓p < 0.0001(n = 9)
MO: [pre-post F(1, 34) = 63.29, p < 0.0001]				
Threshold (mV)	MBG	↑p < 0.0001(n = 26)	↑p < 0.005(n = 10)	↑p < 0.05(n = 14)
CA1: [pre-post F(1, 54) = 221.0, p < 0.0001]	Oua	↑p < 0.0001(n = 21)	↑p < 0.0001(n = 15)	p = 0.649(n.s) (n = 14)
PTL: [pre-post F(1, 30) = 88.75, p < 0.0001]	Comb	↑p < 0.0001(n = 10)	↑p < 0.0001(n = 8)	↑p < 0.0001(n = 9)
MO: [pre-post F(1, 34) = 25.283, p < 0.0001]				
Amplitude (mV)	MBG	↓p < 0.0001(n = 26)	↓p < 0.0001(n = 10)	↓p < 0.0001(n = 14)
CA1: [pre-post F(1, 54) = 200.2, p < 0.0001]	Oua	↓p < 0.0001(n = 21)	↓p < 0.0001(n = 15)	p = 0.370(n.s) (n = 14)
PTL: [pre-post F(1, 30) = 124.7, p < 0.0001]	Comb	↓p < 0.0001(n = 10)	↓p < 0.0001(n = 8)	↓p < 0.0001(n = 9)
MO: [pre-post F(1, 34) = 78.33, p < 0.0001]				
Width (msec.)	MBG	p = 0.094(n.s) (n = 26)	↑p < 0.005(n = 10)	↑p < 0.0001(n = 14)
CA1: [pre-post F(1, 54) = 255.0, p < 0.0001]	Oua	↑p < 0.0001(n = 21)	↑p < 0.0001(n = 15)	p = 0.597(n.s) (n = 14)
PTL: [pre-post F(1, 30) = 65.20, p < 0.0001]	Comb	↑p < 0.0001(n = 10)	↑p < 0.0001(n = 8)	↑p < 0.0001(n = 9)
MO: [pre-post F(1, 34) = 53.99, p < 0.0001]				
dV/dt (V/Sec)	MBG	↓p < 0.0001(n = 26)	↓p < 0.005(n = 10)	↓p < 0.0001(n = 14)
CA1: [pre-post F(1, 54) = 175.1, p < 0.0001]	Oua	↓p < 0.0001(n = 21)	↓p < 0.0001(n = 15)	p = 0.597(n.s) (n = 14)
PTL: [pre-post F(1, 30) = 68.67, p < 0.0001]	Comb	↓p < 0.0001(n = 9)	↓p < 0.0001(n = 8)	↓p < 0.0001(n = 9)
MO: [pre-post F(1, 34) = 48.37, p < 0.0001]				
AUC (mV × msec.)	MBG	p = 0.305(n.s) (n = 26)	↑p < 0.05(n = 10)	↑p < 0.0001(n = 14)
CA1: [pre-post F(1, 54) = 74.23, p < 0.0001]	Oua	↑p < 0.0001(n = 21)	↑p < 0.0001(n = 15)	p = 0.301(n.s) (n = 14)
PTL: [pre-post F(1, 30) = 39.38, p < 0.0001]	Comb	↑p < 0.0001(n = 10)	↑p < 0.0001(n = 8)	↑p < 0.0001(n = 9)
MO: [pre-post F(1, 34) = 54.443, p < 0.0001]				
mAHP (mV)	MBG	p = 0.334(n.s) (n = 14)	↓p < 0.0001(n = 10)	↓p < 0.0001(n = 12)
CA1: [pre-post F(1, 42) = 44.546, p < 0.0001]	Oua	↓p < 0.0001(n = 21)	↓p < 0.0001(n = 15)	p = 0.109(n.s) (n = 14)
PTL: [pre-post F(1, 30) = 135.9, p < 0.0001]	Comb	↓p < 0.0001(n = 10)	↓p < 0.0001(n = 8)	↓p < 0.0001(n = 7)
MO: [pre-post F(1, 30) = 125.89, p < 0.0001]				
eEPSC (mV)	MBG	p = 0.828(n.s) (n = 9)	p = 0.806(n.s)(n = 10)	↓p < 0.0001(n = 11)
CA1: [pre-post F(1, 37) = 111.8, p < 0.0001]	Oua	↓p < 0.0001(n = 21)	↓p < 0.0001(n = 15)	p = 0.383(n.s)(n = 14)
PTL: [pre-post F(1, 30) = 51.05, p < 0.0001]	Comb	↓p < 0.0001(n = 10)	↓p < 0.0001(n = 8)	↓p < 0.0001(n = 9)
MO: [pre-post F(1, 31) = 87.2, p < 0.0001]				
AP Frequency (Hz)	MBG	↑p < 0.001(n = 26)	↓p < 0.05(n = 10)	↓p < 0.001(n = 14)
CA1: [pre-post F(1, 54) = 130.690, p < 0.0001]	Oua	↓p < 0.001(n = 21)	↓p < 0.01(n = 15)	p = 0.69(n.s) (n = 14)
PTL: [pre-post F(1, 30) = 20.726, p < 0.0001]	Comb	↓p < 0.001(n = 10)	↓p < 0.001(n = 8)	↓p < 0.001(n = 9)
MO: [pre-post F(1, 34) = 300.319, p < 0.0001]				

The electrophysiological properties of cells are compared before (ACSF) and after the application of a specific NaKA inhibitor. The values presented are of one-way Repeated Measure ANOVA results with sphericity assumed corrections. (n = number of cells recorded). Arrowheads indicate the effect direction compared to ACSF baseline.

depressed the firing index similar to MBG and Oua combination, (p < 0.001, RM-ANOVA) (Fig. 4) (see Table 3).

Taken together, these results showed that with regard to affecting the FI curve in MO region α1-NaKA plays a dominant role while α3-NaKA is negligible. However, in CA1 there is a bimodal alteration of excitability by α1-NaKA and α3-NaKA inhibition. Inhibition of α3-NaKA induces a partial depression, whereas α1-NaKA inhibition increased excitability (Fig. 4). Interestingly, the combination of inhibiting these two isoforms together, induced a complete depression of the FI curve. The PTL region showed a similar pattern to the one observed in CA1 (Fig. 4).

3.5. Isoform-selective inhibition induced a differential effect on synaptic transmission

To complete the investigation, we determined the effects of isoform-selective NaKA inhibition on synaptic transmission, by applying either MBG or Oua and measured the change in evoked excitatory post-synaptic current (eEPSC). Surprisingly, MBG application did not alter the evoked synaptic response in CA1 and PTL pyramidal cells (p = 0.828 and p = 0.806 respectively, RM-ANOVA);

while Oua application in these two regions induced a significant depression of the eEPSC (p < 0.0001 for both regions, RM-ANOVA) (Fig. 5). However, in MO pyramidal cells, Oua application did not affect synaptic response (p = 0.383, RM-ANOVA), while MBG significantly depressed eEPSC amplitude (p < 0.0001, RM-ANOVA) (Fig. 5) (see Table 2). In addition, a complementary comparison between the two drugs within CA1, showed a robust depression of eEPSC by Oua over MBG, while within MO region MBG had a much stronger depressing effect than Oua (p < 0.0001 for both CA1 and MO, 2-way RM-ANOVA) (see Table 3). Our present findings, regarding Oua, demonstrated that an induced depression of synaptic transmission coincided with the previous studies (Vaillend et al., 2002; Zhang et al., 2009) while the effects of α1-NaKA inhibition on synaptic transmission were never investigated, to the best of our knowledge.

4. Discussion

NaKA plays a major role in brain functionality via its ability to modify synaptic transmission (Hernández-R. and Condés-Lara, 1992; Phillis and Wu, 1981), cellular excitability (Zhang and Sillar,

Table 3
Comparisons between the effects of various selective NaKA inhibitions for each brain region.

Property [Two Way RM-ANOVA, post-hoc Tukey]	drug	CA1sp	PTLpL5	MOpL5
Rp (mV)	**MBG-Oua**	$p < 0.05$	(n.s)	$p < 0.05$
CA1: [Drugs x pre-post $F(2, 54) = 11.23$, $p < 0.0001$]	**MBG-comb**	$p < 0.01$	$p < 0.05$	(n.s)
PTL: [Drugs x pre-post $F(2, 30) = 4.747$, $p < 0.05$]	**Oua-comb**	(n.s)	(n.s)	$p < 0.001$
MO: [Drugs x pre-post $F(2, 34) = 26.01$, $p < 0.0001$]				
IR (mΩ)	**MBG-Oua**	(n.s)	(n.s)	$p < 0.05$
CA1: [Drugs x pre-post $F(2, 54) = 1.400$, $p = 0.2554$ (n.s)]	**MBG-comb**	(n.s)	(n.s)	(n.s)
PTL: [Drugs x pre-post $F(2, 30) = 1.101$, $p = 0.3455$ (n.s)]	**Oua-comb**	(n.s)	(n.s)	(n.s)
MO: [Drugs x pre-post $F(2, 34) = 2.638$, $p = 0.086$ (n.s)]				
Sag (mV)	**MBG-Oua**	$p < 0.001$	(n.s)	$p < 0.0001$
CA1: [Drugs x pre-post $F(2, 54) = 14.89$, $p < 0.0001$]	**MBG-comb**	$p < 0.0001$	$p < 0.001$	(n.s)
PTL: [Drugs x pre-post $F(2, 30) = 6.286$, $p < 0.01$]	**Oua-comb**	(n.s)	(n.s)	$p < 0.0001$
MO: [Drugs x pre-post $F(2, 34) = 13.655$, $p < 0.0001$]				
Threshold (mV)	**MBG-Oua**	$p < 0.05$	(n.s)	(n.s)
CA1: [Drugs x pre-post $F(2, 54) = 19.67$, $p < 0.0001$]	**MBG-comb**	$p < 0.001$	$p < 0.05$	$p < 0.05$
PTL: [Drugs x pre-post $F(2, 30) = 4.538$, $p < 0.05$]	**Oua-comb**	(n.s)	(n.s)	$p < 0.05$
MO: [Drugs x pre-post $F(2, 34) = 6.938$, $p < 0.005$]				
Amplitude (mV)	**MBG-Oua**	$p < 0.01$	(n.s)	$p < 0.01$
CA1: [Drugs x pre-post $F(2, 54) = 15.31$, $p < 0.0001$]	**MBG-comb**	$p < 0.0001$	(n.s)	(n.s)
PTL: [Drugs x pre-post $F(2, 30) = 4.411$, $p < 0.05$]	**Oua-comb**	$p < 0.01$	(n.s)	$p < 0.0001$
MO: [Drugs x pre-post $F(2, 34) = 15.181$, $p < 0.0001$]				
Width (msec.)	**MBG-Oua**	$p < 0.0001$	(n.s)	$p < 0.0001$
CA1: [Drugs x pre-post $F(2, 54) = 72.98$, $p < 0.0001$]	**MBG-comb**	$p < 0.0001$	(n.s)	(n.s)
PTL: [Drugs x pre-post $F(2, 30) = 2.164$, $p = 0.1325$ (n.s)]	**Oua-comb**	$p < 0.0001$	(n.s)	$p < 0.0001$
MO: [Drugs x pre-post $F(2, 34) = 11.459$, $p < 0.0005$]				
dV/dt (V/Sec)	**MBG-Oua**	$p < 0.05$	(n.s)	$p < 0.001$
CA1: [Drugs x pre-post $F(2, 54) = 10.73$, $p < 0.0001$]	**MBG-comb**	$p < 0.0001$	(n.s)	(n.s)
PTL: [Drugs x pre-post $F(2, 30) = 1.727$, $p = 0.1949$ (n.s)]	**Oua-comb**	$p < 0.05$	(n.s)	$p < 0.0001$
MO: [Drugs x pre-post $F(2, 34) = 10.744$, $p < 0.0005$]				
AUC (mV × msec.)	**MBG-Oua**	$p < 0.0001$	(n.s)	$p < 0.0001$
CA1: [Drugs x pre-post $F(2, 54) = 31.03$, $p < 0.0001$]	**MBG-comb**	$p < 0.0001$	(n.s)	(n.s)
PTL: [Drugs x pre-post $F(2, 30) = 1.184$, $p = 0.3198$ (n.s)]	**Oua-comb**	$p < 0.05$	(n.s)	$p < 0.0001$
MO: [Drugs x pre-post $F(2, 34) = 8.852$, $p = 0.001$]				
mAHP (mV)	**MBG-Oua**	$p < 0.01$	(n.s)	$p < 0.0001$
CA1: [Drugs x pre-post $F(2, 42) = 6.776$, $p < 0.005$]	**MBG-comb**	$p < 0.001$	(n.s)	(n.s)
PTL: [Drugs x pre-post $F(2, 30) = 2.738$, $p = 0.081$ (n.s)]	**Oua-comb**	(n.s)	(n.s)	$p < 0.0001$
MO: [Drugs x pre-post $F(2, 30) = 22.55$, $p < 0.0001$]				
EPSC (mV)	**MBG-Oua**	$p < 0.0001$	$p < 0.001$	$p < 0.0001$
CA1: [Drugs x pre-post $F(2, 37) = 23.50$, $p < 0.0001$]	**MBG-comb**	$p < 0.0001$	$p < 0.001$	(n.s)
PTL: [Drugs x pre-post $F(2, 30) = 11.36$, $p < 0.0005$]	**Oua-comb**	$p < 0.01$	(n.s)	$p < 0.0001$
MO: [Drugs x pre-post $F(2, 31) = 18.130$, $p < 0.0001$]				
AP Frequency (Hz)	**MBG-Oua**	$p < 0.001$	$p < 0.001$	$p < 0.001$
CA1: [Drugs x pre-post $F(2, 54) = 161.381$, $p < 0.0001$]	**MBG-comb**	$p < 0.001$	$p < 0.001$	(n.s)
PTL: [Drugs x pre-post $F(2, 30) = 21.882$, $p < 0.001$]	**Oua-comb**	$p < 0.001$	(n.s)	$p < 0.001$
MO: [Drugs x pre-post $F(2, 34) = 76.260$, $p < 0.0001$]				

The effects of the selective inhibitors are compared within each brain region. The values presented are of two-way repeated measures ANOVA with post hoc Tukey correction. (n, number of cells).

2012) and/or network excitability (Pulver and Griffith, 2010). In addition, various endogenous CTS are present in the brain in high concentrations, and presumably, affect normal brain function *via* modulation of NaKA activity and structural changes (Nesher et al., 2007). Alterations in NaKA activity are implicated in various neuropsychiatric disorders, as well as learning and memory deficits (Corti et al., 2011; de Lores Arnaiz and Ordieres, 2014; Dickey et al., 2005; Graham et al., 2015; Zhang et al., 2012). Uncovering these intricate interactions and mechanisms of NaKA isoforms is crucial for the effort of resolving many of these pathological conditions. It is also known that most of the pyramidal cells have higher resting NaKA activity and the ability to contain high Na$^+$ loads during active periods (Anderson et al., 2010). Previous studies investigated the role of these NaKA isoforms in behavior, establishing the differential contribution of each isoform to diverse types of behaviors (Lingrel et al., 2007; Moseley et al., 2007). However, possible differences in physiological activity of NaKA with its various α-subunit isoforms in the adult rodent brain have not been thoroughly examined. While there are ample studies characterizing the physiological effects of α3-NaKA inhibition by Oua in a single brain region, inhibition of α1-NaKA was not thoroughly investigated. The

herein study is the first to thoroughly characterize the physiology of both α1-NaKA and α3-NaKA selective inhibition in pyramidal cells, with a systematic comparison between distinct brain regions.

Previous studies showed that in addition to maintaining the internal Na$^+$ and K$^+$ concentrations, NaKA generates an outward current and contributes to a voltage drop in the resting membrane potential (Baylor and Nicholls, 1969; Carpenter and Alving, 1968; Glitsch, 2001; Hodgkin and Keynes, 1955). Thus, the alterations in the passive properties, due to NaKA inhibition and subsequent modification of active intrinsic properties, were expected. However, a prominent observation from our study indicates that α1-NaKA isoform has a dominant role in the motor cortex, while α3-NaKA has a stronger effect at the hippocampal CA1 region. In the present study, the inhibition of either isoform induced significant effects at CA1, but α3-NaKA inhibition had a stronger impact. Notably, α3-NaKA inhibition did not affect layer-5 pyramidal cells in motor cortex (Table 2). These findings are in agreement with a previous, well-constructed, immunohistochemical study that characterized the regional distribution of α3 isoform in the adult mouse brain. Briefly, this previous study demonstrated a milder expression of α3 isoform occurred in the rostral part of the brain, specifically motor
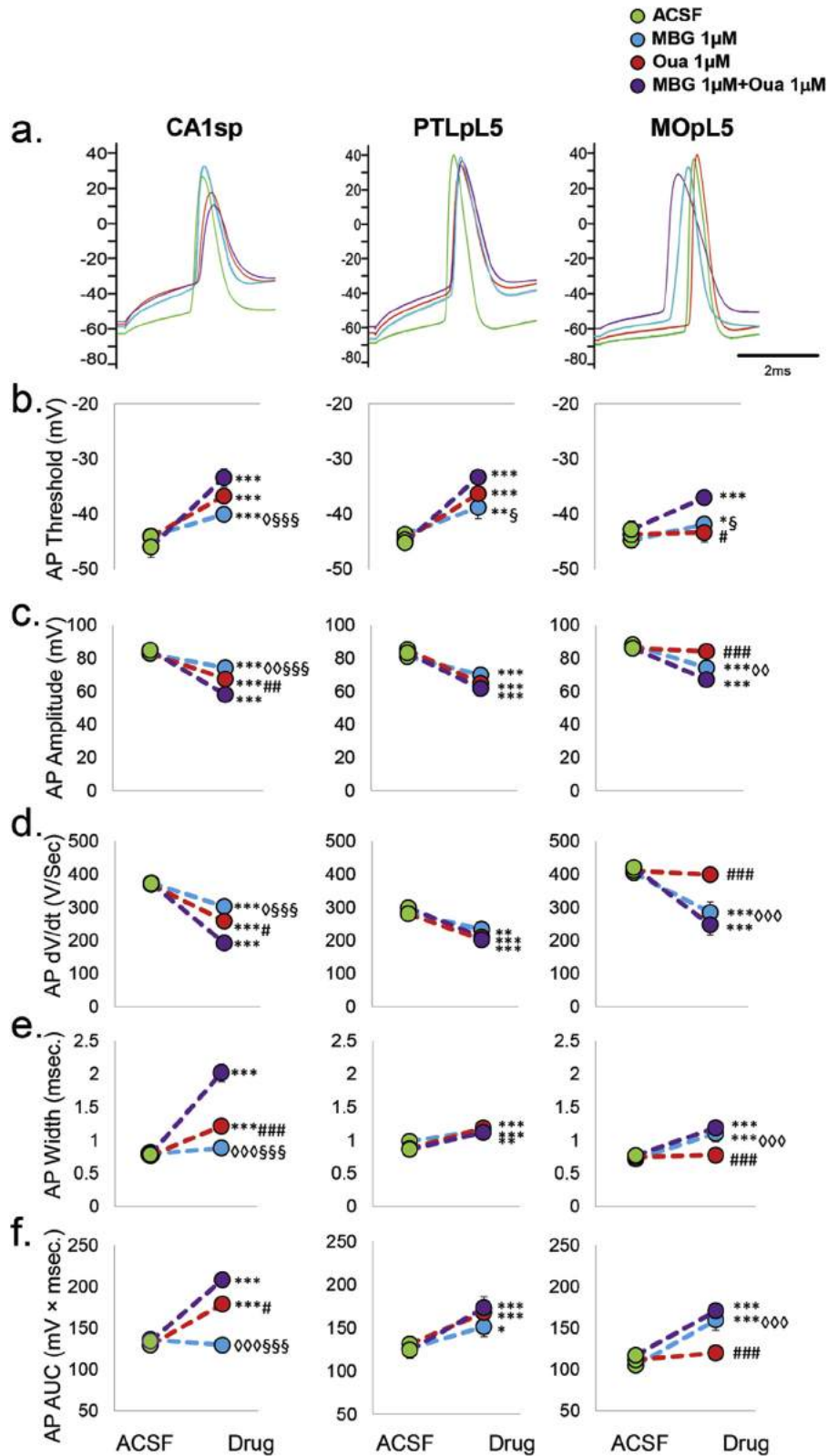
Fig. 2. Selective NaKA inhibition differentially alters action potential properties. **(a)** Overlapped action potential sample traces in response to intracellular current steps injection for 10 ms. **(b)** NaKA inhibition significantly depolarizes the threshold potentials in all three regions. The effect of MBG significantly less than the effect of Oua and Comb in CA1 (Left). In PTLpL5 effect of MBG is considerably less than the effect of Comb (Middle). Notably, Oua does not alter the threshold potential in MOpL5 (Right) and is significantly less than the Comb. **(c–d)** NaKA inhibition reduces AP amplitude, and AP rise slope (AP dV/dt). In comparison to the effect of Comb, MBG and Oua in CA1sp and Oua in MOpL5 exert significantly less effect. On the contrary, in PTLpL5, all NaKA inhibition reduces AP amplitude and rise slope to the same extent (Middle) **(e–f)** In CA1sp the effect of Oua and Comb significantly increases AP width and AP area under curve (AUC) compared with ACSF or MBG. MBG does not alter AP width and AUC. Moreover, the effect of Oua is less than the effect of Comb in CA1 (Left). Whereas, in PTLpL5 all the NaKA inhibition increases AP width and AP AUC to a similar range (Middle). In the case of MOpL5, Oua does not alter the AP width or AUC than ACSF, and its effect is significantly less than the effect of MBG and Comb (Right). Significant differences were marked as follows: *(p < 0.05), **(p < 0.01), ***(p < 0.001) differences between ACSF (green) and drugs applied. ◊(p < 0.05), ◊◊(p < 0.01), ◊◊◊(p < 0.001) for MBG(blue) vs Oua (red), §(p < 0.05), §§(p < 0.01), §§§(p < 0.001) for MBG (blue) vs Comb (purple). #(p < 0.05), ##(p < 0.01), ###(p < 0.001) used for Oua(red) vs Comb (purple). Significance calculated by repeated measure ANOVA, multiple comparisons Tukey Corrections with p < 0.05 (Detailed in Tables 2 and 3) and the values in the graphs are Mean ± SEM.
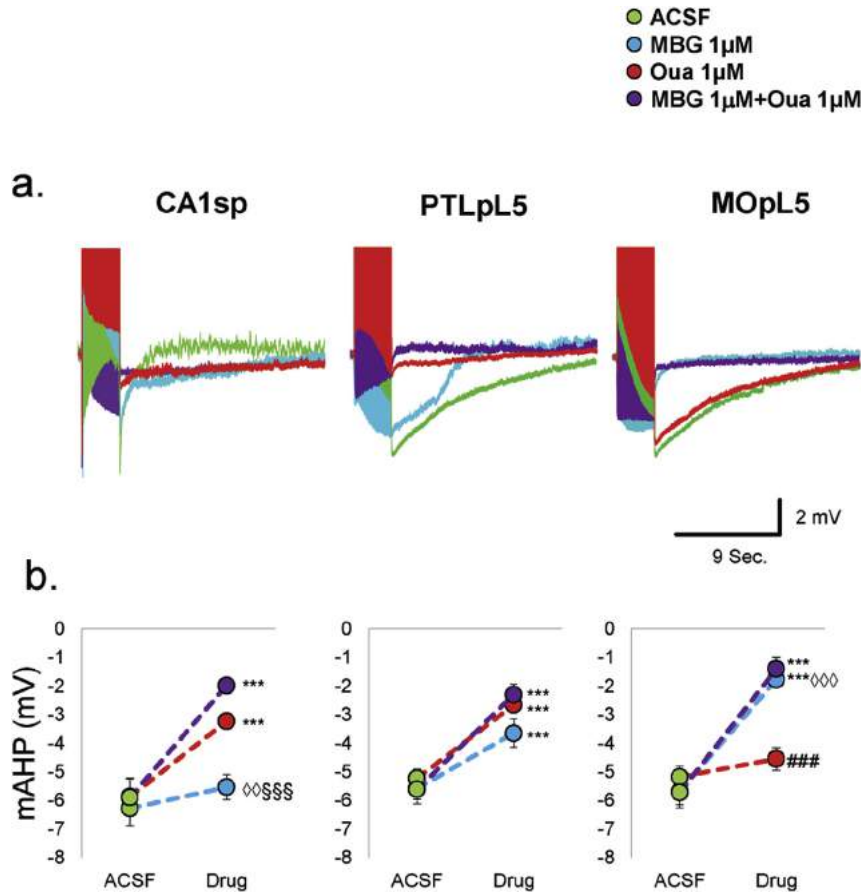
Fig. 3. Effect of selective NaKA inhibition on mAHP. **(a)** Representative traces show that NaKA inhibition reduces mAHP. **(b)** While the effect of MBG in CA1sp is not significantly different from ACSF, but significantly different than the effect of Oua and Comb (Left). In PTLpL5 all the drugs reduced the mAHP than the ACSF, and there is no difference between the effects of the drugs (Middle). However, in MOpL5 the effect of Oua is significantly less than the effect of MBG and Comb with no significant difference with ACSF (Right). Significant differences were marked as before: *($p < 0.05$), **($p < 0.01$) and ***($p < 0.001$) for differences between ACSF(green) and drugs applied. ◊($p < 0.05$), ◊◊($p < 0.01$) and ◊◊◊($p < 0.001$) for MBG(blue) vs Oua (red), §($p < 0.05$), §§($p < 0.01$), §§§($p < 0.001$) for MBG (blue) and Comb (purple). #($p < 0.05$), ##($p < 0.01$), ###($p < 0.001$) used for Oua(red) vs Comb (purple). Significance calculated by repeated measure ANOVA, multiple comparisons, Tukey Corrections with $p < 0.05$ (Detailed in Tables 2 and 3) and the values in the graphs are Mean $\pm$ SEM.

cortex layer 5, and the expression intensified throughout the caudal region as in primary somatosensory cortex and hippocampus (Bøttger et al., 2011). Similarly, *in-situ* hybridization studies in rats showed that $\alpha 3$-NaKA mRNA expression is higher than the $\alpha 1$-NaKA mRNA in the hippocampal CA1 and parietal cortex pyramidal cells (Chauhan et al., 1997; Chauhan and Siegel, 1996). In contrast to the studies investigating $\alpha 3$-NaKA, the few works that investigated $\alpha 1$ isoform expression did not determine conclusive information regarding its regional expression throughout the brain (Hieber et al., 1991; McGrail et al., 1991). Nevertheless, NaKA isoforms expression profiles cannot be the sole explanation for the observed differences between MBG and Oua. All studies, including our own (Kaphzan et al., 2011), showed that both isoforms are expressed in all regions. Therefore, it was a surprising finding in our study, that the motor cortex, which expresses $\alpha 3$-NaKA to some extent, was physiologically insensitive to $\alpha 3$-NaKA inhibition. Interestingly, we demonstrated that selective inhibition of a particular NaKA isoform in a specific brain region affected some distinct physiological properties; while other properties were unchanged (e.g. $\alpha 1$-NaKA inhibition at PTL affected mAHP but did not affect synaptic response). Moreover, inhibition of each of the two isoforms in the same brain region exhibited the opposite effects (e.g. $\alpha 1$-NaKA vs. $\alpha 3$-NaKA inhibition in CA1 concerning FI curve).

Altogether, our present data demonstrated that the effects of inhibiting two α-NaKA isoforms are different in distinct brain regions, which indicate the variable mechanisms for their mode of action, and are not result of the differential expressions.

It is well established that the Na^+ pump regulates mAHP in mammalian CA1 and neocortical layer 5 pyramidal neurons (Gustafsson and Wigström, 1983, 1981; Koike et al., 1972), more-than-likely *via* increased pump activity by elevated intracellular Na^+ (Gage and Hubbard, 1966; Lombardo et al., 2004; Pulver and Griffith, 2010). Also, at physiological temperature, NaKA is the principle contributor for mAHP compared to Ca^{+2} (Gulledge et al., 2013). Moreover, the inhibition of NaKA with Oua, abolished the AHP in *Xenopus laevis* tadpoles spinal cord central pattern generator neurons (Zhang and Sillar, 2012), which is greatly relevant to our present study. In accordance with this, our present results depicted a strong reduction in CA1 mAHP after $\alpha 3$-NaKA inhibition with Oua, but it was completely unaltered after $\alpha 1$-NaKA inhibition, in spite of significant effects on various intrinsic properties at CA1. Conversely, inhibition of $\alpha 1$-NaKA in the motor cortex decreased mAHP while $\alpha 3$-NaKA inhibition did not alter mAHP (Fig. 3 and Table 2). These findings are an important addition to the previous studies that emphasized the role of NaKA in the regulation of mAHP and suggested differential roles of NaKA isoforms in different brain
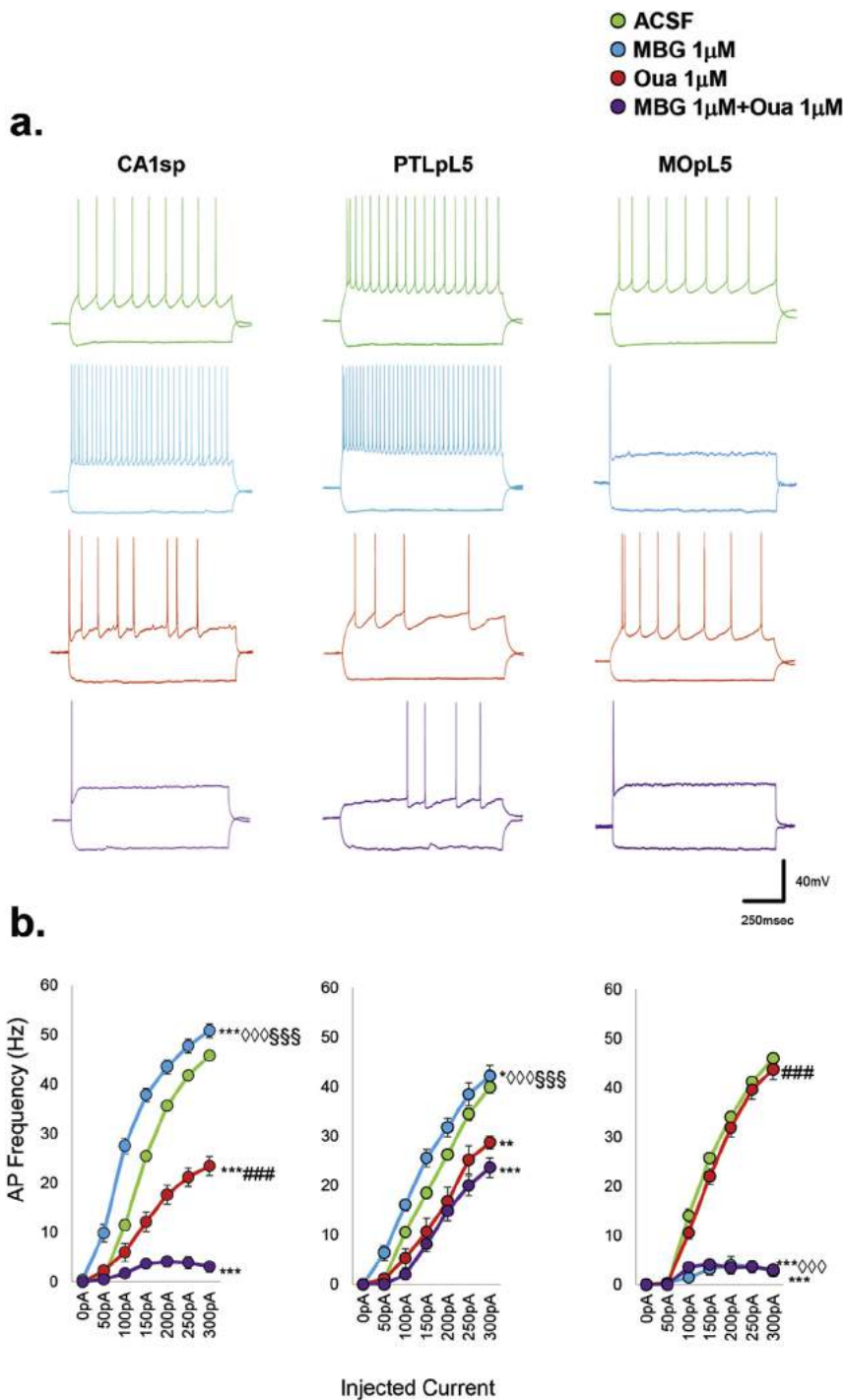
Fig. 4. AP firing frequencies altered with selective NaKA inhibition. **(a)** Sample traces in response to the intracellular current steps (-100 pA and $+150$ pA for 1 s) in all three regions before and after application of drugs, indicating similarity in response in CA1sp and PTLpL5, however, the different response in MOpL5. **(b)** In CA1 and PTLpL5, MBG significantly increases the firing frequency than ACSF while Oua and Comb reduce it. In contrast to PTLpL5, in CA1, the effect of Oua is significantly less than the effect of Comb (Left and Middle). In MOpL5 the application of Oua does not alter the FI, but MBG and Oua reduce it. The effect of MBG and Comb are not different in MOpL5 (Right). Significant differences were marked as before: *($p < 0.05$), **($p < 0.01$) and ***($p < 0.001$) for differences between ACSF(green) and drugs applied. ◊($p < 0.05$), ◊◊($p < 0.01$) and ◊◊◊($p < 0.001$) for MBG (blue) vs Oua (red), §§§($p < 0.001$) for MBG (blue) and Comb (purple). ###($p < 0.05$) used for Oua(red) vs Comb (purple). Significance calculated by two-way repeated measure ANOVA, Huynh-Feldt Correction, multiple comparisons, Tukey Corrections with $p < 0.05$ (Detailed in Tables 2 and 3) and the values in the diagrams are Mean ± SEM.

regions.

In the present study, the firing frequency (FI) modification by selective NaKA inhibition was also puzzling. The layer-5 pyramidal cells in motor cortex are impervious to Oua, and are predominated by α1-NaKA. While in CA1 the effects of the drugs are more complex. Inhibition of α3-NaKA in CA1 reduced excitability, while inhibition of α1-NaKA enhanced excitability. Remarkably, the combination of two inhibitors did not neutralize each other. Instead, a nearly complete depression of almost all firing activity occurred (Fig. 4). This is in accordance with the recent study, which
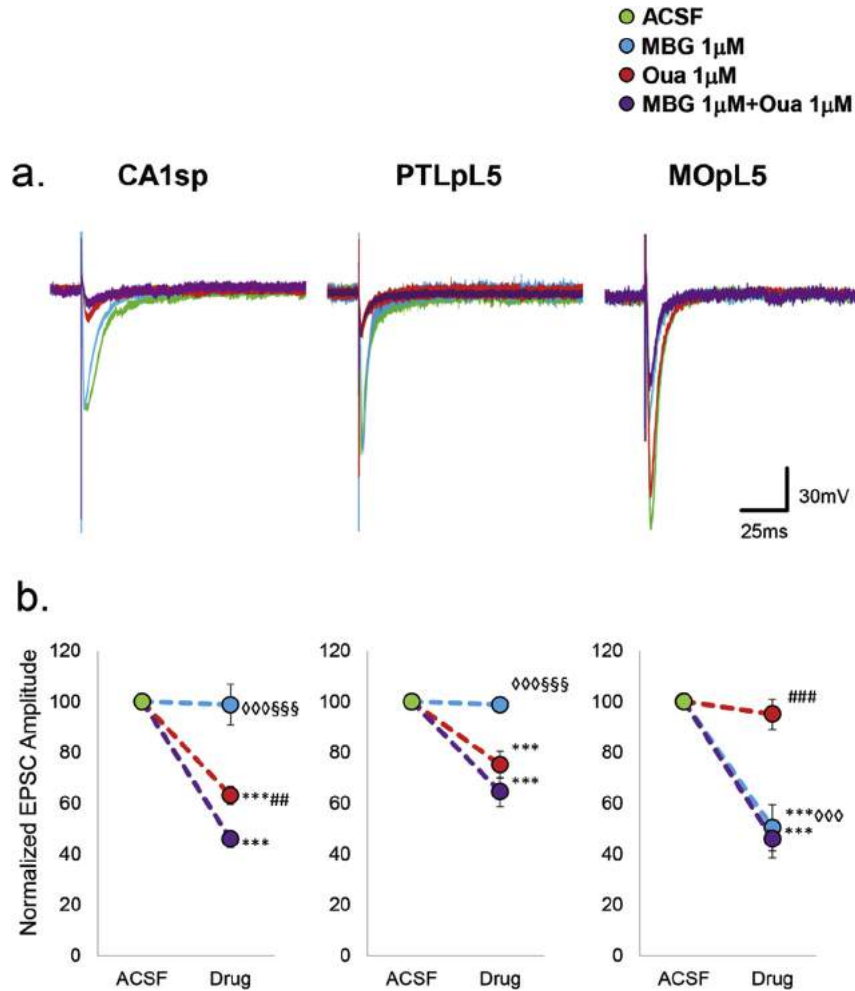
Fig. 5. Effect of NaKA inhibition in EPSC amplitude. **(a)** Voltage clamp recordings in response to applied synaptic stimulations before and after application of drugs in all three regions. Note MBG does not alter the evoked response in CA1sp and PTLpL5 than ACSF. The normalized EPSC amplitude response is shown in (b). In CA1sp and PTLpL5, Oua and Comb significantly reduce the synaptic response, and that is significantly different from the effect of MBG (Left and Middle). While Oua does not diminish the evoked synaptic response in MOpL5 compared to ACSF, thus the effect is significantly less than the effect of MBG and Comb (Right). Significant differences were marked as before: ***(p < 0.001) for differences between ACSF(green) and drugs applied. ◊◊◊(p < 0.001) for MBG(blue) vs Oua (red), §§§(p < 0.001) for MBG (blue) and Comb (purple). ##(p < 0.01), ###(p < 0.001) used for Oua(red) vs Comb (purple). Significance calculated by repeated measure ANOVA, multiple comparisons, Tukey Corrections with p < 0.05 (Detailed in Tables 2 and 3) and the values in the graphs are Mean ± SEM.

demonstrated MBG synergistic effects, when it was applied in combination with Oua in rat arteries and neurons (Song et al., 2014). The suggested mechanism, underlying this synergistic effect is that MBG binding reduces NaKA activity and alters NaKA transmembrane structural organization, consequently increasing Oua binding efficiency to NaKA. Interestingly, the binding of MBG itself is mostly related to its concentration, rather than to the structural conformation of NaKA. Thus, MBG binding to NaKA increases Oua binding efficiency and potentiates its inhibitory activity *via* the aforementioned mechanism (Klimanova et al., 2015; Schoner, 2002).

In addition, it is suggested that complete arrest of any NaKA activity induces a high amount of neurotransmitter release and evokes a spreading anoxic depolarization (AD) leading to a transient breakdown of neuronal function, with the massive failure of ion homeostasis (Somjen, 2001; White et al., 2012). Altogether, this statement suggested distinctive roles for the various NaKA isoforms in determining cellular excitability and support a possible synergism between them.

Another interesting previous finding is how selectively NaKA

inhibition affects the synaptic response. Previous studies showed that Na^+ pump activity can modify the release of several neurotransmitters (Hernández-R. and Condés-Lara, 1992; Phillis and Wu, 1981). In our results, while layer-5 pyramidal cells at motor cortex were unaffected by α3-NaKA inhibition, the CA1 and layer-5 parietal cortex showed a significant reduction in evoked EPSC. This is in accordance with other studies which demonstrated the reduced field excitatory post-synaptic potentials by using dihydroouabain (another cardiac glycoside like Oua) as an α3-NaKA inhibitor (Vaillend et al., 2002). The underlying mechanisms for synaptic effects of NaKA inhibition are intriguing. It was shown that incubation of rat primary cortical neuron cultures with Oua (50 μM) induced a decrease in the expression of membrane-bound AMPA receptors *via* receptor internalization, and subsequent degradation by the proteasome (Zhang et al., 2009). However, this high Oua concentration is not selective and is expected to bind both NaKA isoforms. In our experimental setup, selective α3-NaKA inhibition by Oua (1 μM) reduced eEPSC, but selective α1-NaKA inhibition by MBG (1 μM) did not alter the evoked synaptic response. These results cannot be explained by the lack of α1-NaKA expression in CA1

or differential subcellular NaKA isoform localization, because MBG significantly altered many other parameters at the CA1 region, such as intrinsic properties and firing frequency.

Furthermore, the combination of MBG and Oua elicited a synergistic effect in depressing the synaptic response. This strong synergism might be due to binding of these two CTS in distinct depths of NaKA and causing varied structural changes in the enzyme molecule (Klimanova et al., 2015). Consequently, these structural modifications not only initiate different signaling cascades, but also may alter the affinity to regulatory proteins (Lauf et al., 2015; Morrill et al., 2012), and thus might affect cellular and synaptic activity.

Such structural interactions may have significant and special roles in neurons. For example, NMDA directly interacts with both α1 and α3 (Akkuratov et al., 2015), and AMPA interacts selectively with α1 (Zhang et al., 2009). On the functional level, NMDA activation differentially altered NaKA activity in a dose-dependent manner while CTS application reduced NMDA expression (Akkuratov et al., 2015), and reduced AMPA expression in a proteasome-dependent manner (Zhang et al., 2009). Additional molecular effects might be indirect. For example, Oua-induced structural alterations stimulate intracellular calcium oscillation via IP3 receptors (Mikoshiba, 2007), which in themselves also reduce the NMDA receptor levels. Another point to consider is that a growing body of research suggests that NaKA may function differently in pyramidal cells, interneurons and glia at the neocortex, and hippocampus (Anderson et al., 2010; McGrail et al., 1991; Richards et al., 2007; Ross and Soltesz, 2000). Such differential NaKA expression may modulate network activity in response to CTS exposure. Nevertheless, our findings were produced in isolated brain slices where network activity is minimal, and the physiological alterations were observed in a gradual increasing pattern at very early time points of stimulation, which makes it less likely to be network effects. On the subcellular level, α1 and α3 isoforms localized expressions are not differently distributed, and both are quite similarly present in pyramidal cell somas, dendrites and axons (Azarias et al., 2013; Pietrini et al., 1992).

To conclude, our data indicated that primarily the α1 isoform determines the NaKA activity and function in rostral brain regions, while α3 NaKA, conducts the same in caudal parts. Furthermore, these differences are found both at rest and during periods of high cellular activity. In addition, we showed that the functionality of the two α-NaKA subunits differ in distinct brain areas and suggest variable mechanisms for the two isoforms and a synergism between them. We also suggest the variable roles for endogenous CTS, MBG and Oua, in normal brain function, and we posit that different endogenous CTS bind to the distinct NaKA isoforms in concert, and participate in modifying brain activity. This designates the endogenous CTS as important molecules associated with learning and memory, as-well-as other brain functions. Nevertheless, the analogy to humans is more complicated. Interestingly, cardiotonic steroids affinity to NaKA subunits are not universal for all of the species; rodent α1 NaKA is inhibited by ouabain and other cardiotonic steroids (CTS) at 10^3-fold higher concentrations than those effective in other mammals. This differential affinity between species is probably the unique feature of α1 NaKA. However, the binding affinities to CTS of both α2 and α3 NaKA isoforms are very similar between rodents and humans (Akimova et al., 2015; Lingrel, 2010). In any case, differential regional effects between the isoforms and the synergism between the two isoforms might still exist and play a role in humans. Thus, increasing interest in the functional implication of NaKA isoforms and endogenous CTS in cellular activity, memory maintenance and disease conditions require further investigation of their differential physiological contribution.

Conflicts of interest

The authors declare that they have no conflicts of interest with the contents of this article.

Appendix A. Supplementary data

Supplementary data related to this article can be found at http://dx.doi.org/10.1016/j.neuropharm.2017.02.016.

References

Agmon, A., Connors, B.W., 1991. Thalamocortical responses of mouse somatosensory (barrel) cortexin vitro. Neuroscience 41, 365–379. http://dx.doi.org/10.1016/0306-4522(91)90333-J.

Akimova, O.A., Tverskoi, A.M., Smolyaninova, L.V., Mongin, A.A., Lopina, O.D., La, J., Dulin, N.O., Orlov, S.N., 2015. Critical role of the α1-Na+, K+–ATPase subunit in insensitivity of rodent cells to cytotoxic action of ouabain. Apoptosis 20, 1200–1210. http://dx.doi.org/10.1007/s10495-015-1144-y.

Akkuratov, E.E., Lopacheva, O.M., Kruusmägi, M., Lopachev, A.V., Shah, Z.A., Boldyrev, A.A., Liu, L., December 2015. Functional interaction between Na/K-ATPase and NMDA receptor in cerebellar neurons. Mol. Neurobiol. 52 (3), 1726–1734. http://dx.doi.org/10.1007/s12035-014-8975-3.

Al-Mosalem, O.A., El-Ansary, A., Attas, O., Al-Ayadhi, L., 2009. Metabolic biomarkers related to energy metabolism in Saudi autistic children. Clin. Biochem. 42, 949–957. http://dx.doi.org/10.1016/j.clinbiochem.2009.04.006.

Allen Institute for Brain Science, 2015. Allen Mouse Brain Atlas [WWW Document]. n.d.

Ames, A., November 2000. CNS energy metabolism as related to function. Brain Res. Rev. 34 (1–2), 42–68. http://dx.doi.org/10.1016/S0165-0173(00).

Anderson, T.R., Huguenard, J.R., Prince, D. a, 2010. Differential effects of Na+-K+ ATPase blockade on cortical layer V neurons. J. Physiol. 588, 4401–4414. http://dx.doi.org/10.1113/jphysiol.2010.191858.

Attwell, D., Laughlin, S.B., 2001. An energy budget for signaling in the grey matter of the brain. J. Cereb. Blood Flow. Metab. 21, 1133–1145. http://dx.doi.org/10.1097/00004647-200110000-00001.

Azarias, G., Kruusmagi, M., Connor, S., Akkuratov, E.E., Liu, X.L., Lyons, D., Brismar, H., Broberger, C., Aperia, A., 2013. A specific and essential role for Na,K-ATPase alpha3 in neurons co-expressing alpha1 and alpha3. J. Biol. Chem. 288, 2734–2743. http://dx.doi.org/10.1074/jbc.M112.425785.

Bagrov, A.Y., Shapiro, J.I., Fedorova, O.V., 2009. Endogenous cardiotonic steroids: physiology, pharmacology, and novel therapeutic targets. Pharmacol. Rev. 61, 9–38. http://dx.doi.org/10.1124/pr.108.000711.

Baylor, D.A., Nicholls, J.G., 1969. Changes in extracellular potassium concentration produced by neuronal activity in the central nervous system of the leech. J. Physiol. 203, 555–569. http://dx.doi.org/10.1113/jphysiol.1969.sp008879.

Blanco, G., Mercer, R.W., 1998. Isozymes of the Na-K-ATPase: heterogeneity in structure, diversity in function. Am. J. Physiol. 275, F633–F650.

Bøttger, P., Tracz, Z., Heuck, A., Nissen, P., Romero-Ramos, M., Lykke-Hartmann, K., 2011. Distribution of Na/K-ATPase alpha 3 isoform, a sodium-potassium P-type pump associated with rapid-onset of dystonia parkinsonism (RDP) in the adult mouse brain. J. Comp. Neurol. 519, 376–404. http://dx.doi.org/10.1002/cne.22524.

Carpenter, D.O., Alving, B.O., 1968. A contribution of an electrogenic Na+ pump to membrane potential in Aplysia neurons. J. Gen. Physiol. 52, 1–21. http://dx.doi.org/10.1085/jgp.52.1.1.

Chagnac-Amitai, Y., Luhmann, H.J., Prince, D.A., 1990. Burst generating and regular spiking layer 5 pyramidal neurons of rat neocortex have different morphological features. J. Comp. Neurol. 296, 598–613. http://dx.doi.org/10.1002/cne.902960407.

Chauhan, N.B., Lee, J.M., Siegel, G.J., 1997. Na,K-ATPase mRNA levels and plaque load in Alzheimer's disease. J. Mol. Neurosci. 9, 151–166. http://dx.doi.org/10.1007/BF02800498.

Chauhan, N.B., Siegel, G.J., 1996. In situ analysis of Na, K-ATPase alpha1- and alpha3-isoform mRNAs in aging rat hippocampus. J. Neurochem. 66, 1742–1751.

Chen, W., Zhang, J.-J., Hu, G.-Y., Wu, C.-P., 1996. Electrophysiological and morphological properties of pyramidal and nonpyramidal neurons in the cat motor cortex in vitro. Neuroscience 73, 39–55. http://dx.doi.org/10.1016/0306-4522(96)00009-7.

Chetcuti, A., Adams, L.J., Mitchell, P.B., Schofield, P.R., 2008. Microarray gene expression profiling of mouse brain mRNA in a model of lithium treatment. Psychiatr. Genet. 18, 64–72. http://dx.doi.org/10.1097/YPG.0b013e3282fb0051.

Christophe, E., Doerflinger, N., Lavery, D.J., Molnár, Z., Charpak, S., Audinat, E., 2005. Two populations of layer v pyramidal cells of the mouse neocortex: development and sensitivity to anesthetics. J. Neurophysiol. 94, 3357–3367. http://dx.doi.org/10.1152/jn.00076.2005.

Colbert, C.M., Levy, W.B., 1992. Electrophysiological and pharmacological characterization of perforant path synapses in CA1: mediation by glutamate receptors. J. Neurophysiol. 68, 1–8.

Corti, C., Xuereb, J.H., Crepaldi, L., Corsi, M., Michielin, F., Ferraguti, F., 2011. Altered levels of glutamatergic receptors and Na+/K+ ATPase-α1 in the prefrontal cortex of subjects with schizophrenia. Schizophr. Res. 128, 7–14. http://dx.doi.org/10.1016/j.schres.2011.01.021.

de Lores Arnaiz, G.R., Ordieres, M.G.L., 2014. Brain Na(+), K(+)-ATPase activity in aging and disease. Int. J. Biomed. Sci. 10, 85–102.

DeTomaso, A.W., Blanco, G., Mercer, R.W., 1994. The alpha and beta subunits of the Na,K-ATPase can assemble at the plasma membrane into functional enzyme. J. Cell Biol. 127, 55–69. http://dx.doi.org/10.1083/jcb.127.1.55.

Dickey, C.A., Gordon, M.N., Wilcock, D.M., Herber, D.L., Freeman, M.J., Morgan, D., 2005. Dysregulation of Na+/K+ ATPase by amyloid in APP+PS1 transgenic mice. BMC Neurosci. 6, 7. http://dx.doi.org/10.1186/1471-2202-6-7.

Erecińska, M., Silver, I.A., 1994. Ions and energy in mammalian brain. Prog. Neurobiol. 43, 37–71. http://dx.doi.org/10.1016/0301-0082(94)90015-9.

Fedorova, O.V., Bagrov, a Y., 1997. Inhibition of Na/K ATPase from rat aorta by two Na/K pump inhibitors, ouabain and marinobufagenin: evidence of interaction with different alpha-subunit isoforms. Am. J. Hypertens. 10, 929–935. https://doi.org/10.1016/S0895-7061(97)00096-4.

Fedorova, O.V., Talan, M.I., Agalakova, N.I., Lakatta, E.G., Bagrov, A.Y., 2002. Endogenous ligand of alpha(1) sodium pump, marinobufagenin, is a novel mediator of sodium chloride–dependent hypertension. Circulation 105, 1122–1127. https://doi.org/10.1161/hc0902.104710.

Fedorova, O.V., Zhuravin, I.A., Agalakova, N.I., Yamova, L.A., Talan, M.I., Lakatta, E.G., Bagrov, A.Y., 2007. Intrahippocampal microinjection of an exquisitely low dose of ouabain mimics NaCl loading and stimulates a bufadienolide Na/K-ATPase inhibitor. J. Hypertens. 25, 1834–1844. http://dx.doi.org/10.1097/HJH.0b013e328200497a.

Forrest, M.D., 2014. The sodium-potassium pump is an information processing element in brain computation. Front. Physiol. 5, 1–4. http://dx.doi.org/10.3389/fphys.2014.00472.

Forrest, M.D., Wall, M.J., Press, D.A., Feng, J., 2012. The sodium-potassium pump controls the intrinsic firing of the cerebellar purkinje neuron. PLoS One 7, e51169. http://dx.doi.org/10.1371/journal.pone.0051169.

Franceschetti, S., Buzio, S., Sancini, G., Panzica, F., Avanzini, G., 1993. Expression of intrinsic bursting properties in neurons of maturing sensorimotor cortex. Neurosci. Lett. 162, 25–28. http://dx.doi.org/10.1016/0304-3940(93)90551-U.

Gage, P.W., Hubbard, J.I., 1966. The origin of the post-tetanic hyperpolarization of mammalian motor nerve terminals. J. Physiol. 184, 335–352. http://dx.doi.org/10.1113/jphysiol.1966.sp007918.

Giese, K.P., Storm, J.F., Reuter, D., Fedorov, N.B., Shao, L.-R., Leicher, T., Pongs, O., Silva, A.J., 1998. Reduced K+ channel inactivation, spike broadening, and afterhyperpolarization in kvβ1.1-deficient mice with impaired learning. Learn. Mem. 5, 257–273. http://dx.doi.org/10.1101/lm.5.4.257.

Glitsch, H.G., 2001. Electrophysiology of the sodium-potassium-ATPase in cardiac cells. Physiol. Rev. 81, 1791–1826. http://dx.doi.org/10.1006/jmcc.1998.0889.

Goldstein, I., Levy, T., Galili, D., Ovadia, H., Yirmiya, R., Rosen, H., Lichtstein, D., 2006. Involvement of Na(+), K(+)-ATPase and endogenous digitalis-like compounds in depressive disorders. Biol. Psychiatry 60, 491–499. http://dx.doi.org/10.1016/j.biopsych.2005.12.021.

Graham, S.F., Nasarauddin, M. Bin, Carey, M., McGuinness, B., Holscher, C., Kehoe, P.G., Love, S., Passmore, A.P., Elliott, C.T., Meharg, A., Green, B.D., 2015. Quantitative measurement of [Na+] and [K+] in postmortem human brain tissue indicates disturbances in subjects with Alzheimer's disease and dementia with Lewy bodies. J. Alzheimers. Dis. 44, 851–857. http://dx.doi.org/10.3233/JAD-141869.

Guan, D., Armstrong, W.E., Foehring, R.C., 2015. Electrophysiological properties of genetically-identified layer 5 neocortical pyramidal neurons: Ca2+-dependence and differential modulation by norepinephrine. J. Neurophysiol. 2014–2032. http://dx.doi.org/10.1152/jn.00524.2014.

Gulledge, A.T., Dasari, S., Onoue, K., Stephens, E.K., Hasse, J.M., Avesar, D., 2013. A sodium-pump-mediated afterhyperpolarization in pyramidal neurons. J. Neurosci. 33, 13025–13041. http://dx.doi.org/10.1523/JNEUROSCI.0220-13.2013.

Gustafsson, B., Wigström, H., 1983. Hyperpolarization following long-lasting tetanic activation of hippocampal pyramidal cells. Brain Res. 275, 159–163. http://dx.doi.org/10.1016/0006-8993(83)90429-8.

Gustafsson, B., Wigström, H., 1981. Evidence for two types of afterhyperpolarization in CA1 pyramidal cells in the hippocampus. Brain Res. 206, 462–468. http://dx.doi.org/10.1016/0006-8993(81)90548-5.

Hernández-R, J., Condés-Lara, M., 1992. Brain Na+/K+-ATPase regulation by serotonin and norepinephrine in normal and kindled rats. Brain Res. 593, 239–244. http://dx.doi.org/10.1016/0006-8993(92)91313-4.

Herrera, V.L., Emanuel, J.R., Ruiz-Opazo, N., Levenson, R., Nadal-Ginard, B., 1987. Three differentially expressed Na,K-ATPase alpha subunit isoforms: structural and functional implications. J. Cell Biol. 105, 1855–1865. http://dx.doi.org/10.1083/jcb.105.4.1855.

Hieber, V., Siegel, G.J., Fink, D.J., Beaty, M.W., Mata, M., 1991. Differential distribution of (Na, K)-ATPase alpha isoforms in the central nervous system. Cell. Mol. Neurobiol. 11, 253–262. http://dx.doi.org/10.1007/BF00769038.

Hodgkin, A.L., Keynes, R.D., 1955. Active transport of cations in giant axons from *Sepia* and *Loligo*. J. Physiol. 128, 28–60. http://dx.doi.org/10.1113/jphysiol.1955.sp005290.

Howarth, C., Gleeson, P., Attwell, D., 2012. Updated energy budgets for neural computation in the neocortex and cerebellum. J. Cereb. Blood Flow. Metab. 32, 1222–1232. http://dx.doi.org/10.1038/jcbfm.2012.35.

Jamme, I., Petit, E., Gerbi, A., Maixent, J.-M., MacKenzie, E.T., Nouvelot, A., 1997. Changes in ouabain affinity of Na+,K+-ATPase during focal cerebral ischaemia in the mouse. Brain Res. 774, 123–130. http://dx.doi.org/10.1016/S0006-8993(97)81695-2.

Ji, L., Chauhan, A., Brown, W.T., Chauhan, V., 2009. Increased activities of Na+/K+-ATPase and Ca2+/Mg2+-ATPase in the frontal cortex and cerebellum of autistic individuals. Life Sci. 85, 788–793. http://dx.doi.org/10.1016/j.lfs.2009.10.008.

Kaphzan, H., Buffington, S.A., Jung, J.I., Rasband, M.N., Klann, E., 2011. Alterations in intrinsic membrane properties and the axon initial segment in a mouse model of angelman syndrome. J. Neurosci. 31, 17637–17648. http://dx.doi.org/10.1523/JNEUROSCI.4162-11.2011.

Kaphzan, H., Buffington, S. a, Ramaraj, A.B., Lingrel, J.B., Rasband, M.N., Santini, E., Klann, E., 2013. Genetic reduction of the α1 subunit of Na/K-ATPase corrects multiple hippocampal phenotypes in angelman syndrome. Cell Rep. 4, 405–412. http://dx.doi.org/10.1016/j.celrep.2013.07.005.

King, B., Rizwan, A.P., Asmara, H., Heath, N.C., Engbers, J.D.T., Dykstra, S., Bartoletti, T.M., Hameed, S., Zamponi, G.W., Turner, R.W., 2015. IKCa channels are a critical determinant of the slow AHP in CA1 pyramidal neurons. Cell Rep. 11, 175–182. http://dx.doi.org/10.1016/j.celrep.2015.03.026.

Klimanova, E.A., Yu, I., Mitkevich, V.A., Anashkina, A.A., Orlov, S.N., Makarov, A.A., Lopina, O.D., 2015. Binding of ouabain and marinobufagenin leads to different structural changes in Na, K-ATPase and depends on the enzyme conformation. FEBS Lett. 50, 1–7. http://dx.doi.org/10.1016/j.febslet.2015.08.011.

Koike, H., Mano, N., Okada, Y., Oshima, T., 1972. Activities of the sodium pump in cat pyramidal tract cell studied with intracellular injection of sodium ions. Exp. Brain Res. 14, 449–462.

Kueh, D., Barnett, W.H., Cymbalyuk, G.S., Calabrese, R.L., 2016. Na(+)/K(+) pump interacts with the h-current to control bursting activity in central pattern generator neurons of leeches. Elife 5, e19322. http://dx.doi.org/10.7554/eLife.19322.

Lacaille, J.C., Mueller, A.L., Kunkel, D.D., Schwartzkroin, P. a, 1987. Local circuit interactions between oriens/alveus interneurons and CA1 pyramidal cells in hippocampal slices: electrophysiology and morphology. J. Neurosci. 7, 1979–1993.

Landfield, P., Pitler, T., 1984. Prolonged Ca2+-dependent afterhyperpolarizations in hippocampal neurons of aged rats. Sci. (80-.) 226, 1089–1092. http://dx.doi.org/10.1126/science.6494926.

Lauf, P.K., Alqahtani, T., Flues, K., Meller, J., Adragna, N.C., 2015. Interaction between Na-K-ATPase and Bcl-2 proteins BclXL and bak. Am. J. Physiol. Cell Physiol. 308, C51–C60. http://dx.doi.org/10.1152/ajpcell.00287.2014.

Laughery, M.D., Clifford, R.J., Chi, Y., Kaplan, J.H., 2007. Selective basolateral localization of overexpressed Na-K-ATPase beta1- and beta2- subunits is disrupted by butyrate treatment of MDCK cells. Am. J. Physiol. Ren. Physiol. 292, F1718–F1725. http://dx.doi.org/10.1152/ajprenal.00360.2006.

Lein, E.S., Hawrylycz, M.J., Ao, N., Ayres, M., Bensinger, A., Bernard, A., Boe, A.F., Boguski, M.S., Brockway, K.S., Byrnes, E.J., Chen, L., Chen, L., Chen, T.-M., Chin, M.C., Chong, J., Crook, B.E., Czaplinska, A., Dang, C.N., Datta, S., Dee, N.R., Desaki, A.L., Desta, T., Diep, E., Dolbeare, T.A., Donelan, M.J., Dong, H.-W., Dougherty, J.G., Duncan, B.J., Ebbert, A.J., Eichele, G., Estin, L.K., Faber, C., Facer, B.A., Fields, R., Fischer, S.R., Fliss, T.P., Frensley, C., Gates, S.N., Glattfelder, K.J., Halverson, K.R., Hart, M.R., Hohmann, J.G., Howell, M.P., Jeung, D.P., Johnson, R.A., Karr, P.T., Kawal, R., Kidney, J.M., Knapik, R.H., Kuan, C.L., Lake, J.H., Laramee, A.R., Larsen, K.D., Lau, C., Lemon, T.A., Liang, A.J., Liu, Y., Luong, L.T., Michaels, J., Morgan, J.J., Morgan, R.J., Mortrud, M.T., Mosqueda, N.F., Ng, L.L., Ng, R., Orta, G.J., Overly, C.C., Pak, T.H., Parry, S.E., Pathak, S.D., Pearson, O.C., Puchalski, R.B., Riley, Z.L., Rockett, H.R., Rowland, S.A., Royall, J.J., Ruiz, M.J., Sarno, N.R., Schaffnit, K., Shapovalova, N.V., Sivisay, T., Slaughterbeck, C.R., Smith, S.C., Smith, K.A., Smith, B.I., Sodt, A.J., Stewart, N.N., Stumpf, K.-R., Sunkin, S.M., Sutram, M., Tam, A., Teemer, C.D., Thaller, C., Thompson, C.L., Varnam, L.R., Visel, A., Whitlock, R.M., Wohnoutka, P.E., Wolkey, C.K., Wong, V.Y., Wood, M., Yaylaoglu, M.B., Young, R.C., Youngstrom, B.L., Yuan, X.F., Zhang, B., Zwingman, T.A., Jones, A.R., 2007. Genome-wide atlas of gene expression in the adult mouse brain. Nature 445, 168–176. http://dx.doi.org/10.1038/nature05453.

Lescale-Matys, L., Putnam, D.S., McDonough, A.A., 1993. Na(+)-K(+)-ATPase alpha 1- and beta 1-subunit degradation: evidence for multiple subunit specific rates. Am. J. Physiol. 264, C583–C590.

Lingrel, J.B., 2010. The physiological significance of the cardiotonic steroid/ouabain-binding site of the Na,K-ATPase. Annu. Rev. Physiol. 72, 395–412. http://dx.doi.org/10.1146/annurev-physiol-021909-135725.

Lingrel, J.B., Williams, M.T., Vorhees, C.V., Moseley, A.E., 2007. Na,K-ATPase and the

role of alpha isoforms in behavior. J. Bioenerg. Biomembr. 39, 385—389. http://dx.doi.org/10.1007/s10863-007-9107-9.

Lingrel, J.B., 1992. Na, K-ATPase : isoform structure, function, and expression. J. Bioenerg. Biomembr. 24, 263—270.

Lombardo, P., Scuri, R., Cataldo, E., Calvani, M., Nicolai, R., Mosconi, L., Brunelli, M., 2004. Acetyl-l-carnitine induces a sustained potentiation of the after-hyperpolarization. Neuroscience 128, 293—303. http://dx.doi.org/10.1016/j.neuroscience.2004.06.028.

McDonough, A.A., Farley, R.A., 1993. Regulation of Na,K-ATPase activity. Curr. Opin. Nephrol. Hypertens. 2, 725—734.

McGrail, K.M., Phillips, J.M., Sweadner, K.J., 1991. Immunofluorescent localization of three Na,K-ATPase isozymes in the rat central nervous system: both neurons and glia can express more than one Na,K-ATPase. J. Neurosci. 11, 381—391.

Mikoshiba, K., 2007. IP3 receptor/Ca2+ channel: from discovery to new signaling concepts. J. Neurochem. 102, 1426—1446. http://dx.doi.org/10.1111/j.1471-4159.2007.04825.x.

Mircheff, A.K., Bowen, J.W., Yiu, S.C., McDonough, A.A., 1992. Synthesis and trans-location of Na(+)-K(+)-ATPase alpha- and beta-subunits to plasma membrane in MDCK cells. Am. J. Physiol. 262, C470—C483.

Moeller, H.B., Olesen, E.T.B., Fenton, R.A., 2011. Regulation of the water channel aquaporin-2 by posttranslational modification. AJP Ren. Physiol. 300, F1062—F1073. http://dx.doi.org/10.1152/ajprenal.00721.2010.

Mogul, D.J., Singer, D.H., Ten Eick, R.E., 1990. Dependence of Na-K pump current on internal Na+ in mammalian cardiac myocytes. Am. J. Physiol. 259, H488—H496.

Morrill, G.A., Kostellow, A.B., Askari, A., 2012. Caveolin-Na/K-ATPase interactions: role of transmembrane topology in non-genomic steroid signal transduction. Steroids 77, 1160—1168. http://dx.doi.org/10.1016/j.steroids.2012.04.012.

Moseley, A.E., Williams, M.T., Schaefer, T.L., Bohanan, C.S., Neumann, J.C., Behbehani, M.M., Vorhees, C.V., Lingrel, J.B., 2007. Deficiency in Na,K-ATPase alpha isoform genes alters spatial learning, motor activity, and anxiety in mice. J. Neurosci. 27, 616—626. http://dx.doi.org/10.1523/JNEUROSCI.4464-06.2007.

Munzer, J.S., Daly, S.E., Jewell-Motz, E. a, Lingrel, J.B., Blostein, R., 1994. Tissue- and isoform-specific kinetic behavior of the Na,K-ATPase. J. Biol. Chem. 269, 16668—16676.

Nesher, M., Shpolansky, U., Rosen, H., Lichtstein, D., 2007. The digitalis-like steroid hormones: new mechanisms of action and biological significance. Life Sci. 80, 2093—2107. http://dx.doi.org/10.1016/j.lfs.2007.03.013.

Oh, M.M., Oliveira, F. a., Disterhoft, J.F., 2010. Learning and aging related changes in intrinsic neuronal excitability. Front. Aging Neurosci. 2, 1—10. http://dx.doi.org/10.3389/neuro.24.002.2010.

Phillis, J.W., Wu, P.H., 1981. The role of adenosine and its nucleotides in central synaptic transmission. Prog. Neurobiol. 16, 187—239. http://dx.doi.org/10.1016/0301-0082(81)90014-9.

Pietrini, G., Matteolif, M., Banker, G., Caplan, M.J., Hoffman, J.F., 1992. Isoforms of the Na,K-ATPase are present in both axons and dendrites of hippocampal neurons in culture. Cell Biol. 89, 8414—8418.

Power, J.M., Wu, W.W., Sametsky, E., Oh, M.M., Disterhoft, J.F., 2002. Age-related enhancement of the slow outward calcium-activated potassium current in hippocampal CA1 pyramidal neurons in vitro. J. Neurosci. 22, 7234—7243 doi: 20026641.

Pulver, S.R., Griffith, L.C., 2010. Spike integration and cellular memory in a rhythmic network from Na+/K+ pump current dynamics. Nat. Neurosci. 13, 53—59. http://dx.doi.org/10.1038/nn.2444.

Richards, K.S., Bommert, K., Szabo, G., Miles, R., 2007. Differential expression of Na+/K+-ATPase alpha-subunits in mouse hippocampal interneurones and py-ramidal cells. J. Physiol. 585, 491—505. http://dx.doi.org/10.1113/jphysiol.2007.144733.

Ross, S.T., Soltesz, I., 2000. Selective depolarization of interneurons in the early posttraumatic dentate gyrus: involvement of the Na(+)/K(+)-ATPase. J. Neurophysiol. 83, 2916—2930.

Sakai, R., Hagiwara, N., Matsuda, N., Kassanuki, H., Hosoda, S., 1996. Sodium—potassium pump current in rabbit sino-atrial node cells. J. Physiol. 490, 51—62. http://dx.doi.org/10.1113/jphysiol.1996.sp021126.

Schoner, W., 2002. Endogenous cardiac glycosides, a new class of steroid hormones. Eur. J. Biochem. 269, 2440—2448. http://dx.doi.org/10.1046/j.1432-1033.2002.02911.x.

Schubert, D., Staiger, J.F., Cho, N., Kotter, R., Zilles, K., Luhmann, H.J., 2001. Layer-specific intracolumnar and transcolumnar functional connectivity of layer V pyramidal cells in rat barrel cortex. J. Neurosci. 21, 3580—3592.

Schwindt, P.C., Spain, W.J., Foehring, R.C., Chubb, M.C., Crill, W.E., 1988. Slow con-ductances in neurons from cat sensorimotor cortex in vitro and their role in slow excitability changes. J. Neurophysiol. 59, 450—467.

Somjen, G.G., 2001. Mechanisms of spreading depression and hypoxic spreading depression-like depolarization. Physiol. Rev. 81, 1065—1096.

Song, H., Karashima, E., Hamlyn, J.M., Blaustein, M.P., 2014. Ouabain-digoxin antagonism in rat arteries and neurones. J. Physiol. 592, 941—969. http://dx.doi.org/10.1113/jphysiol.2013.266866.

Staff, N.P., Jung, H.Y., Thiagarajan, T., Yao, M., Spruston, N., 2000. Resting and active properties of pyramidal neurons in subiculum and CA1 of rat hippocampus. J. Neurophysiol. 84, 2398—2408.

Tokhtaeva, E., Sachs, G., Vagin, O., 2009. Assembly with the Na,K-ATPase alpha(1) subunit is required for export of beta(1) and beta(2) subunits from the endo-plasmic reticulum. Biochemistry 48, 11421—11431. http://dx.doi.org/10.1021/bi901438z.

Vaillend, C., Mason, S.E., Cuttle, M.F., Alger, B.E., 2002. Mechanisms of neuronal hyperexcitability caused by partial inhibition of Na+-K+-ATPases in the rat CA1 hippocampal region. J. Neurophysiol. 88, 2963—2978. http://dx.doi.org/10.1152/jn.00244.2002.

Wang, Y.-C., Yang, J.-J., Huang, R.-C., 2012. Intracellular Na(+) and metabolic mod-ulation of Na/K pump and excitability in the rat suprachiasmatic nucleus neurons. J. Neurophysiol. 108, 2024—2032. http://dx.doi.org/10.1152/jn.00361.2012.

White, S.H., Brisson, C.D., Andrew, R.D., 2012. Examining protection from anoxic depolarization by the drugs dibucaine and carbetapentane using whole cell recording from CA1 neurons. J. Neurophysiol. 107, 2083—2095. http://dx.doi.org/10.1152/jn.00701.2011.

Wu, W.W., Chan, C.S., Disterhoft, J.F., 2004. Slow afterhyperpolarization governs the development of NMDA receptor-dependent afterdepolarization in CA1 pyra-midal neurons during synaptic stimulation. J. Neurophysiol. 92, 2346—2356. http://dx.doi.org/10.1152/jn.00977.2003.

Zahler, R., Zhang, Z.T., Manor, M., Boron, W.F., 1997. Sodium kinetics of Na,K-ATPase alpha isoforms in intact transfected HeLa cells. J. Gen. Physiol. 110, 201—213.

Zhang, D., Hou, Q., Wang, M., Lin, A., Jarzylo, L., Navis, A., Raissi, A., Liu, F., Man, H.-Y.H.-Y., 2009. Na,K-ATPase activity regulates AMPA receptor turnover through proteasome-mediated proteolysis. J. Neurosci. 29, 4498—4511. http://dx.doi.org/10.1523/JNEUROSCI.6094-08.2009.

Zhang, H.-Y., Sillar, K.T., 2012. Report short-term memory of motor network per-formance via activity-dependent potentiation of Na +/K + pump function. Curr. Biol. 22, 526—531. http://dx.doi.org/10.1016/j.cub.2012.01.058.

Zhang, L.N., Su, S.W., Guo, F., Guo, H.C., Shi, X.L., Li, W.Y., Liu, X., Wang, Y.L., 2012. Serotonin-mediated modulation of Na+/K+ pump current in rat hippocampal CA1 pyramidal neurons. BMC Neurosci. 13, 10. http://dx.doi.org/10.1186/1471-2202-13-10.